

## A PHOTOMETRIC SEARCH FOR HALO BINARIES. II. RESULTS

BRUCE W. CARNEY<sup>a)</sup>

Department of Physics and Astronomy, University of North Carolina, Chapel Hill, North Carolina 27514

Received 29 November 1982

## ABSTRACT

We present the results of a search for binaries in 71 halo dwarf stars, plus a few other dwarfs of special interest. The technique involves metallicity-insensitive blue versus infrared colors, and is based on *uvbyUBVRJJK* photometry, much of which was presented in the preceding paper. Two of the four known binaries, one of the five previously suggested radial velocity variables, and five new candidates are detected. Given that the method's binary detection efficiency is about 50%, we conclude the halo dwarf binary frequency may be as high as 20%–25%. In three appendices we discuss some other valuable results of such extensive photometry: the dwarfs' temperature scale, bolometric corrections, and reddening determinations for stars with  $4500 \leq T_{\text{eff}} \leq 7000$  K.

## I. INTRODUCTION

Binaries among stars of the disk population are common to the point of majority (Abt 1979), but what about the halo stars? Oort (1926) first pointed out that the fraction of double stars is two to three times lower among the high-velocity stars. In fact, in his classical paper describing Populations I and II, Baade (1944) acknowledged that Oort's work was the first to suggest the existence of two distinct stellar populations. In this paper we will review some of the searches for halo binaries and present evidence for some new candidates based in part on the photometric data of the preceding paper (Carney 1983; hereafter referred to as Paper II).

The identification of halo binaries is an important observational task for two primary reasons. First, the low-metallicity mass-luminosity relation has not yet been empirically determined. A calibration of this relation would have significant impact on modelling integrated stellar populations and especially in determining the halo stars' helium abundance via stellar structure modelling. For such ancient stars, this helium abundance should approximate that produced by the Big Bang. Second, since a major difference between the halo and disk populations is the dynamical state of the protostellar matter (Eggen, Lynden-Bell, and Sandage 1962), an observed difference in the binary frequencies would indicate how important dynamics and perhaps metallicity are to binary formation.

Searches for halo binaries have been undertaken in both domains in which halo stars are found: the field and the globular clusters. In the clusters, one is able to study many stars with the same metallicity (excluding  $\omega$  Cen), and searches have been made for eclipsing binaries

and radial velocity variables. The "primordial" binary fraction in globular clusters is difficult to determine, however, because of continuing binary disruption and formation, but the binary fraction is an important datum in the clusters' dynamical evolution. Trimble (1980) has excellently reviewed the interplay of theory and observation of binaries in clusters and we will not discuss it further.

Among the field halo stars, results of systematic searches for radial velocity variability have been published by Abt and Levy (1969), and by Crampton and Hartwick (1972). Of the 19 very metal-poor stars covered by these two programs, no obvious binaries were discovered. There are several known halo binaries, however, such as HD 103095 (see Beardsley, Gatewood, and Kamper 1974), HD 111980 and HD 149414 (see Mayor and Turon 1982), HD 163810 (ADS 10938A), and HD 219617 (ADS 16644). Worley (1969) has published a list of 18 known and suggested subdwarf binaries, although in several cases (HD 6582, HD 23439, SS Cyg) the stars are not metal deficient enough to qualify as extreme halo stars. New halo binary candidates are occasionally suggested, primarily based on radial velocity data. Sandage (1969), for example, listed nine suspected-to-certain radial velocity variables. Follow-up work for these stars has regrettably materialized slowly. G9-16 (BD + 25°1981) is a binary and a blue straggler (Carney and Peterson 1981b). G17-25 (HD 149414) has been extensively studied by Mayor and Turon (1982). G26-9 (BD - 0°4234) has been found to be old disk double-lined binary (Peterson *et al.* 1980), rather like an RS CVn or BY Dra system. Except for this last star and the only moderately metal-poor G88-31 (HD 59374), we will later discuss the stars in Sandage's list. In addition, we briefly note two metal-poor radial velocity variables in the southern hemisphere, HD 29907 and HD 89499, as well as HD 211998 ( $\nu$  Ind), which is metal poor, has a parallax indicating it is a subgiant, and has been claimed

<sup>a)</sup> Visiting Astronomer, Kitt Peak National Observatory, which is operated by AURA, Inc., under contract with the National Science Foundation.

TABLE I. Photometric data.

Star	V	B-V	U-V	V-R <sub>J</sub>	V-I <sub>J</sub>	V-J	V-H	V-K	b-y	m <sub>1</sub>	c <sub>1</sub>	M <sub>0</sub> ( $\pi$ )
HD 3567	9.25	+0.46	+0.31	+0.46	+0.79	+1.04	+1.32	+1.35	+0.330	+0.086	+0.278	3.25 ± 5.97
BD + 71°31	10.26	+0.37	+0.20	+0.52	+0.87	+1.07	+1.32	+1.34	+0.309	+0.040	+0.360	5.51 ± 0.65
HD 4307	6.16	+0.60	+0.66	+0.59	+1.01	+1.16	+1.46	+1.52	+0.387	+0.185	+0.347	
HD 5996	7.67	+0.75	+1.04	+0.605	+1.02	+1.32	+1.68	+1.74				
HD 6582	5.16	+0.70	+0.80	+0.65	+1.14	+1.40	+1.76	+1.82	+0.434	+0.211	+0.216	5.73 ± 0.02
HD 6755	7.72	+0.72	+0.79	+0.65	+1.14	+1.545	+1.97	+2.04	+0.478	+0.103	+0.319	
HD 7424	10.08	+0.75	+0.75	+0.54	+0.91	+1.22	+1.58	+1.64				
HD 7983	8.90	+0.59	+0.565	+0.54	+0.91	+1.17	+1.49	+1.53	[+0.396	+0.116	+0.376]	6.49 ± 0.39
BD + 72°94	10.20	+0.38	+0.17	+0.54	+0.88	+1.30	+1.55	+1.60	+0.309	+0.087	+0.263	
HD 13043	6.89	+0.62	+0.77	+0.52	+0.91	+1.12	+1.42	+1.46	[+0.394	+0.174	+0.479]	4.67 ± 0.42
BD + 29°366	8.76	+0.575	+0.485	+0.56	+0.95	+1.18	+1.50	+1.55	[+0.389	+0.099	+0.335]	3.61 ± 0.72
HD 13403	7.00	+0.65	+0.76	+0.52	+0.90	+1.24	+1.59	+1.63	0.406	+0.220	+0.352	4.65 ± 1.17
BD - 1°306	9.08	+0.57	+0.495	+0.57	+0.95	+1.15	+1.465	+1.52	+0.377	+0.132	+0.224	4.81 ± 0.87
HD 13783	8.30	+0.67	+0.77	+0.57	+0.95	+1.26	+1.63	+1.67				
HD 16031	9.78	+0.44	+0.23	+0.51	+0.87	+1.00	+1.27	+1.31	+0.323	+0.086	+0.257	
HD 16397	7.35	+0.585	+0.585	+0.51	+0.87	+1.14	+1.45	+1.49	+0.382	+0.175	+0.260	5.19 ± 0.59
BD + 9°352	10.18	+0.44	+0.19	+0.47	+0.82	+1.085	+1.36	+1.415	+0.343	+0.070	+0.240	
G4 - 37	11.415	+0.47	+0.26	+0.47	+0.82	+1.095	+1.38	+1.415	[+0.346	+0.044	+0.365]	4.66 ± 0.62
HD 19445	8.05	+0.46	+0.22	+0.54	+0.89	+1.06	+1.35	+1.39	+0.349	+0.052	+0.200	5.94 ± 0.51
HD 20619	7.05	+0.65	+0.755	+0.60	+0.99	+1.18	+1.52	+1.56	+0.406	+0.214	+0.262	6.64 ± 0.50
HD 20727	8.47	+0.68	+0.85	+0.60	+0.99	+1.325	+1.72	+1.77				
BD + 11°468	10.78	+0.54	+0.38	+0.61	+1.04	+1.22	+1.54	+1.59	[+0.393	+0.090	+0.241]	6.72 ± 0.66
BD + 66°268	9.91	+0.66	+0.56	+0.74	+1.28	+1.39	+1.76	+1.835	+0.442	+0.077	+0.165	
HD 21581	8.71	+0.83	+1.04	+0.54	+0.89	+1.71	+2.20	+2.285	+0.549	+0.133	+0.331	
HD 22879	6.695	+0.54	+0.455	+0.505	+0.845	+1.12	+1.435	+1.465	+0.360	+0.132	+0.265	4.91 ± 0.20
HD 24341	7.89	+0.68	+0.80	+0.59	+0.90	+1.00	+1.325	+1.77				
HD 25329	8.51	+0.865	+1.235	+0.75	+1.27	+1.71	+2.18	+2.275	+0.532	+0.295	+0.218	7.17 ± 0.20
BD + 21°607	9.23	+0.45	+0.25	+0.46	+0.80	+1.01	+1.27	+1.325	[+0.321	+0.072	+0.345]	
HD 29587	7.28	+0.63	+0.67	+0.54	+0.90	+1.23	+1.56	+1.61	+0.390	+0.208	+0.230	4.18 ± 0.54
BD + 3°740	9.81	+0.36	+0.16	+0.52	+0.86	+1.01	+1.275	+1.31	[+0.307	+0.071	+0.434]	
HD 35956	6.75	+0.585	+0.63	+0.52	+0.86	+1.21	+1.54	+1.61	+0.375	+0.188	+0.317	4.71 ± 0.39
BD + 12°853	10.22	+0.65	+0.63	+0.59	+1.01	+1.41	+1.80	+1.88	+0.429	+0.180	+0.176	6.89 ± 0.39
HD 250792	9.30	+0.62	+0.59	+0.59	+1.01	+1.35	+1.74	+1.80				
G102 - 47	10.31	+0.64	+0.59	+0.58	+1.01	+1.43	+1.84	+1.91	+0.447	+0.116	+0.244	
BD + 37°1458	8.92	+0.595	+0.485	+0.58	+1.01	+1.35	+1.73	+1.80	+0.428	+0.079	+0.228	
HD 45282	8.035	+0.66	+0.65	+0.605	+1.045	+1.425	+1.825	+1.905	[+0.456	+0.087	+0.351]	
HD 45391	7.16	+0.615	+0.665	+0.53	+0.89	+1.21	+1.53	+1.58	+0.396	+0.192	+0.259	4.88 ± 0.50
G89 - 13	9.39	+0.90	+1.57	+0.53	+0.89	+1.65	+2.10	+2.18	[+0.510	+0.385	+0.449]	
G89 - 14	10.40	+0.465	+0.275	+0.56	+0.97	+1.11	+1.41	+1.46	[+0.323	+0.084	+0.402]	
BD + 19°1730	10.74	+0.44	+0.25	+0.56	+0.97	+1.05	+1.31	+1.36	+0.331	+0.077	+0.309	
G90 - 3	10.43	+0.48	+0.14	+0.42	+0.70	+1.21	+1.53	+1.57	+0.376	+0.048	+0.304	
BD + 24°1676	10.82	+0.36	+0.14	+0.42	+0.69	+1.01	+1.25	+1.28	+0.298	+0.070	+0.355	
HD 60298	7.35:	+0.655	+0.76	+0.42	+0.69	+1.15	+1.44	+1.50	[+0.388	+0.178	+0.437]	
HD 60778	9.10	+0.10	+0.24	+0.36	+0.97	+0.36	+0.41	+0.43	+0.082	+0.118	+1.27	6.17 ± 0.23
HD 64090	8.27	+0.61	+0.48	+0.56	+0.97	+1.31	+1.67	+1.73	+0.431	+0.117	+0.147	
BD + 80°245	10.07	+0.50	+0.33	+0.545	+0.89	+1.39	+1.75	+1.79	+0.402	+0.082	+0.234	
HD 68017	6.81	+0.68	+0.81	+0.425	+0.74	+1.28	+1.62	+1.68	+0.414	+0.212	+0.278	4.98 ± 0.25
BD + 54°1216	9.69	+0.48	+0.29	+0.42	+0.70	+1.04	+1.315	+1.335	+0.336	+0.078	+0.256	4.21 ± 0.90
HD 70958	5.61	+0.46	+0.395	+0.42	+0.70	+0.94	+1.16	+1.20	+0.311	+0.138	+0.256	4.19 ± 0.21
HD 74000	9.64	+0.42	+0.18	+0.33	+0.69	+0.96	+1.22	+1.26	+0.317	+0.075	+0.298	5.66 ± 0.68
G115 - 22	10.96	+0.58	+0.46	+0.33	+0.525	+1.23	+1.56	+1.61	+0.389	+0.116	+0.177	
BD + 25°1981	9.29	+0.30	+0.16	+0.33	+0.525	+0.73	+0.90	+0.93	+0.233	+0.120	+0.498	
HD 74721	8.70	+0.40	+0.14	+0.33	+0.525	+0.17	+0.19	+0.21	+0.025	+0.144	+1.248	
BD - 12°2669	10.24	+0.30	+0.15	+0.32	+0.515	+0.74	+0.92	+0.92	+0.234	+0.085	+0.539	

TABLE I. (continued)

Star	$V$	$B - V$	$U - V$	$V - R_J$	$V - I_J$	$V - J$	$V - H$	$V - K$	$b - y$	$m_1$	$c_1$	$M_0 (M_\odot)$
HD 76932	5.83	+0.51	+0.44	+0.50	+1.12	+1.42	+1.45	+0.364	+0.123	+0.289	2.34 ± 0.98	
BD - 372525	9.68	+0.48	+0.28	+0.46	+1.14	+1.44	+1.495	[+0.358	+0.081	+0.306]	3.57 ± 2.89	
HD 80218	6.64	+0.47	+0.41	+0.75	+1.02	+1.26	+1.30	[+0.338	+0.138	+0.399	3.54 ± 0.72	
HD 81192	6.52	+0.95	+1.52	+1.28	+1.78	+2.30	+2.37	[+0.589	+0.265	+0.499]		
BD + 972190	11.15	+0.38	+0.18	+0.68	+0.975	+1.235	+1.27	[+0.319	+0.045	+0.420]		
BD + 12341p	10.465	+0.36	+0.135	+0.67	+0.945	+1.175	+1.205	[+0.295	+0.068	+0.355	6.49 ± 0.95	
HD 84937	8.31	+0.17	+0.17	+0.39	+0.93	+1.17	+1.21	[+0.303	+0.065	+0.367	5.30 ± 0.43	
BD + 4471910	10.93	+0.42	+0.22	+0.67	+1.04	+1.32	+1.35	[+0.325	+0.052	+0.345	5.93 ± 2.17	
BD + 581218	9.94	+0.70	+0.73	+0.65	+1.48	+1.94	+2.00	[+0.515	+0.03	+0.445]		
HD 85504	6.01	-0.04	-0.11	+1.14	-0.06	-0.04	-0.06	[+0.017	+0.137	+1.040	0.52 ± 1.09	
HD 86986	7.99	+0.13	+0.285		+0.405	-0.46	-0.46	-0.090	+0.120	+1.263		
HD 87140	8.98	+0.70	+0.72	+1.10	+1.53	+1.95	+2.00	+0.480	+0.115	+0.292		
HD 88609	8.58	+0.94	+1.365	+1.43	+1.83	+2.36	+2.43	+0.657	+0.140	+0.589		
HD 88725	7.73	+0.60	+0.59	+0.87	+1.16	+1.52	+1.57	+0.409	+0.126	+0.325	5.85 ± 0.31	
HD 89125	5.81	+0.50	+0.45	+0.74	+1.005	+1.29	+1.32	+0.336	+0.140	+0.352	4.70 ± 0.18	
HD 90508	6.45	+0.60	+0.66	+0.80	+1.12	+1.47	+1.52	+0.396	+0.180	+0.277	4.99 ± 0.21	
BD + 102179	9.97	-0.18	-1.08	+0.80	-0.41	-0.46	-0.53	[+0.374	+0.060	+0.243]	3.71 ± 1.63	
BD + 292091	10.24	+0.50	+0.27	+0.455	+1.15	+1.45	+1.50	[+0.343	+0.088	+0.260	6.95 ± 0.69	
HD 94028	8.22	+0.48	+0.30	+0.785	+1.07	+1.34	+1.39	[+0.508	+0.125	+0.164]	5.03 ± 0.66	
G10 - 4	11.40	+0.72	+0.705		+1.56	+1.955	+2.045	[+0.314	+0.077	+0.319	8.64 ± 0.54	
BD + 362165	9.76	+0.43	+0.23	+0.415	+0.98	+1.225	+1.27	+0.293	+0.105	+0.409		
HD 97916	9.23	+0.43	+0.30	+0.44	+0.75	+1.16	+1.20	+0.293	+0.105	+0.409		
HD 100363	8.6	+0.29	+0.28	+0.465	+0.94	+1.16	+1.20	+0.293	+0.105	+0.409		
HD 101177	6.46	+0.57	+0.59	+0.80	+1.33	+1.71	+1.74	+0.321	+0.035	+0.454	4.87 ± 0.27	
HD 101606	5.73	+0.43	+0.36	+0.41	+0.92	+1.15	+1.16	[+0.310	+0.125	+0.400	2.97 ± 0.39	
BD + 511696	9.92	+0.55	+0.40	+0.655	+1.23	+1.56	+1.60	+0.392	+0.100	+0.171	6.59 ± 0.12	
HD 103095	6.44	+0.75	+0.915		+1.56	+1.96	+2.02	+0.483	+0.220	+0.170		
HD 105262	7.08	-0.01	-0.06	+1.115	+0.18	+0.25	+0.26	+0.058	+0.048	+1.363		
BD - 43208	10.05	+0.405	+0.20		+1.02	+1.29	+1.31	[+0.46	+0.13	+0.505]	7.39 ± 0.96	
HD 105546	8.61	+0.425	+0.21	+0.465	+1.06	+1.37	+1.37	[+0.354	+0.032	+0.320]	8.06 ± 0.63	
G11 - 44	11.11	+0.47	+0.295	+0.425	+0.955	+1.355	+1.395	[+0.346	+0.073	+0.356]	3.35 ± 0.47	
HD 106038	10.165	+0.47	+0.32	+0.72	+1.33	+1.76	+1.80	[+0.317	+0.115	+0.331	5.50 ± 0.75	
HD 106516	6.115	+0.455	+0.32		+1.06	+1.35	+1.37	+0.323	+0.080	+0.279	7.13 ± 0.49	
HD 107760	8.0b	+0.73	+0.99	+0.455	+1.34	+1.74	+1.80	[+0.442	+0.201	+0.355]	7.33 ± 0.57	
HD 108177	9.67	+0.43	+0.195	+0.78	+1.01	+1.29	+1.32	[+0.325	+0.032	+0.329		
HD 108754	9.02	+0.43	+0.84	+0.61	+1.37	+1.75	+1.81	+0.046	+0.131	+1.288		
BD + 282137	10.91	+0.40	+0.16	+0.455	+1.02	+1.29	+1.32	+0.372	+0.200	+0.149	5.18 ± 1.45	
HD 109995	7.61	+0.04	+0.10	+0.54	+1.02	+1.33	+1.35	[+0.354	+0.078	+0.267]	3.56 ± 1.38	
BD + 73566	9.30	+0.60	+0.52	+0.54	+1.23	+1.54	+1.57	[+0.372	+0.153	+0.351	6.73 ± 0.27	
HD 110897	5.95	+0.55	+0.52	+0.54	+1.09	+1.44	+1.45	+0.354	+0.078	+0.267		
G60 - 48	11.32	+0.48	+0.27	+0.74	+1.13	+1.42	+1.47	[+0.354	+0.078	+0.267]		
HD 114095	8.35	+0.94	+1.50	+0.54	+1.77	+2.35	+2.42	+0.060	+0.114	+1.204		
HD 114606	8.72	+0.62	+0.68	+0.54	+1.59	+1.99	+2.06	+0.301	+0.047	+0.356		
HD 117880	9.05	+0.105	+0.255	+0.405	+0.22	+0.28	+0.26	+0.301	+0.059	+0.361	6.56 ± 0.87	
G64 - 12	11.45	+0.38	+0.15	+0.685	+0.93	+1.19	+1.22	+0.633	+0.090	+0.550		
BD + 342476	10.05	+0.395	+0.19	+0.71	+0.95	+1.21	+1.23	+0.253	+0.132	+0.488	3.47 ± 0.21	
HD 122563	6.20	+0.90	+1.28	+0.42	+1.40	+1.87	+1.97	+0.067	+0.109	+1.262		
HD 123710	8.21	+0.59	+0.52	+0.815	+1.87	+2.43	+2.51	+0.328	+0.067	+0.280		
HD 128167	4.47	+0.37	+0.29	+0.34	+0.85	+1.15	+1.15	[+0.283	+0.105	+0.387]		
HD 130095	8.13	+0.08	+0.14	+0.51	+0.76	+0.95	+0.97	+0.253	+0.132	+0.488		
BD + 262606	9.72	+0.425	+0.195	+0.45	+0.26	+0.33	+0.33	+0.067	+0.109	+1.262		
G66 - 30	11.06	+0.40	+0.23	+0.67	+1.06	+1.34	+1.37	+0.328	+0.105	+0.387]	6.02 ± 0.39	
HD 132142	7.80	+0.78	+1.14	+1.115	+1.56	+1.97	+1.99	+0.386	+0.071	+0.358	5.28 ± 0.69	
HD 132475	8.565	+0.555	+0.42	+0.905	+1.235	+1.585	+1.625					

TABLE I. (continued)

Star	$V$	$B - V$	$U - V$	$V - R_J$	$V - I_J$	$V - J$	$V - H$	$V - K$	$b - y$	$m_1$	$c_1$	$M_0(\pi)$
HD 134169	7.69	+0.535	+0.46	+0.49	+0.825	+1.12	+1.44	+1.46	+0.376	+0.124	+0.305	6.99 ± 0.23
HD 134439	9.09	+0.76	+0.92	+0.69	+1.15	+1.56	+1.99	+2.04	+0.490	+0.191	+0.239	7.36 ± 0.23
HD 134440	9.46	+0.85	+1.18	+0.765	+1.275	+1.71	+2.18	+2.25	+0.531	+0.247	+0.266	
G15 - 23	10.96	+0.71	+0.75			+1.46	+1.86	+1.93	[+0.449	+0.200	+0.137	
G15 - 24	11.44	+0.57	+0.46			+1.21	+1.58	+1.63	[+0.411	+0.090	+0.253]	
HD 140283	7.23	+0.48	+0.27	+0.51	+0.87	+1.24	+1.56	+1.59	+0.377	+0.044	+0.311	6.01 ± 0.34
HD 142267	6.10	+0.58	+0.58	+0.525	+0.88	+1.21	+1.50	+1.52	+0.385	+0.190	+0.254	3.82 ± 0.43
HD 142373	4.62	+0.57	+0.57	+0.48	+0.80	+1.15	+1.46	+1.47	+0.380	+0.158	+0.322	3.36 ± 0.19
BD - 16'4187	10.92	+0.83	+0.99			+1.66	+2.13	+2.22				
HD 144061	7.25	+0.65	+0.70			+1.24	+1.64	+1.64				5.03 ± 0.66
BD + 67'922	9.44	+0.88	+0.20			+2.27	+3.06	+3.19				
BD + 42'2667	9.86	+0.46	+0.26	+0.465	+0.80	+1.03	+1.32	+1.36	+0.338	+0.073	+0.280	3.75 ± 3.26
HD 144579	6.66	+0.73	+0.93	+0.605	+1.025	+1.83	+1.85	+1.85				6.18 ± 0.14
HD 144515	8.28	+0.78	+1.06	+0.69	+1.23	+1.65	+2.24	+2.24				5.18 ± 0.54
G180 - 58	11.29	+0.68	+0.60	+0.485	+0.825	+1.44	+1.83	+1.90	+0.466	+0.107	+0.091	4.52 ± 0.39
HD 148816	7.28	+0.53	+0.46			+1.33	+1.72	+1.78	+0.362	+0.127	+0.320	
BD - 6'4455	10.18	+0.80	+1.02			+1.56	+2.02	+2.09	[+0.475	+0.182	+0.268]	7.85 ± 0.59
HD 149414	9.63	+0.74	+0.84	+0.70	+1.19	+1.49	+1.97	+1.97	+0.374	+0.152	+0.349	4.74 ± 0.36
HD 157089	6.96	+0.58	+0.56	+0.505	+0.855	+1.16	+1.52	+1.54	+0.409	+0.182	+0.309	4.67 ± 0.15
HD 157214	5.38	+0.62	+0.685	+0.51	+0.845	+1.26	+1.65	+1.69				4.76 ± 0.93
HD 158809	8.15	+0.66	+0.72	+0.565	+0.94	+1.12	+1.42	+1.42	[+0.349	+0.041	+0.317]	
BD + 2'3375	9.95	+0.45	+0.21	+0.48	+0.83	+1.14	+1.47	+1.51				
HD 160693	8.41	+0.58	+0.55	+0.52	+0.865	+0.52	+0.63	+0.65				5.94 ± 0.75
HD 161817	6.96	+0.17	+0.315			+1.43	+1.78	+1.87	[+0.455	+0.052	+0.322]	6.35 ± 1.40
BD - 8'4501	10.62	+0.45	+0.45	+0.66	+1.15	+1.55	+1.97	+2.03	[+0.492	+0.051	+0.363]	
HD 161770	9.70	+0.66	+0.62	+0.33	+0.63	+0.89	+1.16	+1.20	[+0.320	+0.058	+0.350]	
BD + 20'3603	9.76	+0.44	+0.255	+0.60	+0.875	+1.33	+1.72	+1.76	[+0.428	+0.056	+0.197]	7.80 ± 1.30
G154 - 34	11.29	+0.69	+0.56			+1.39	+1.83	+1.91				6.14 ± 0.65
HD 163810	9.63	+0.60	+0.52	+0.60	+1.01	+1.39	+1.83	+1.91	+0.882	+0.012	+0.791	4.97 ± 0.25
HD 165195	7.30	+1.29	+2.23	+1.06	+1.87	+2.52	+3.13	+3.26	+0.408	+0.144	+0.276	3.88 ± 0.15
HD 165401	6.80	+0.61	+0.64	+0.51	+0.875	+1.19	+1.50	+1.52	+0.357	+0.137	+0.335	
HD 165908	5.06	+0.52	+0.43	+0.49	+0.83	+1.10	+1.41	+1.43	+0.505	+0.254	+0.290	
HD 170737	8.09	+0.82	+1.17	+0.64	+1.14	+1.55	+2.03	+2.09	+0.336	+0.146	+0.317	4.12 ± 0.08
HD 170153	3.58	+0.49	+0.43	+0.44	+0.75	+1.10	+1.38	+1.40	[+0.499	+0.040	+0.324]	
BD + 13'3683	10.57	+0.64	+0.56			+1.55	+1.97	+2.05	[+0.342	+0.047	+0.317]	7.17 ± 0.47
G206 - 34	11.38	+0.40	+0.15			+1.01	+1.32	+1.34				
BD + 20'3876	9.33	+0.645	+0.725	+0.565	+0.93	+1.27	+1.61	+1.65	[+0.385	+0.123	+0.369]	5.10 ± 0.95
HD 175305	7.18	+0.76	+0.91	+0.66	+1.15	+1.58	+2.02	+2.08				
HD 175179	9.08	+0.58	+0.54	+0.54	+0.89	+1.28	+1.62	+1.63				6.82 ± 0.28
HD 181007	9.595	+0.79	+0.97	+0.725	+1.235	+1.725	+2.225	+2.295				
BD + 41'3306	8.86	+0.81	+0.81	+0.68	+1.20	+1.59	+2.05	+2.13	[+0.317	+0.052	+0.419]	
BD + 26'3578	9.36	+0.39	+0.17	+0.41	+0.74	+0.95	+1.21	+1.24	+0.416	+0.113	+0.614	
HD 184266	7.58	+0.57	+0.67	+0.56	+0.99	+1.31	+1.68	+1.74	+0.390	+0.142	+0.314	4.28 ± 0.38
HD 184499	6.62	+0.58	+0.58	+0.50	+0.86	+1.33	+1.33	+1.34	+0.408	+0.130	+0.12	
HD 188510	8.83	+0.59	+0.47	+0.57	+0.94	+1.28	+1.64	+1.69	[+0.69	+0.045	+0.485]	
BD - 18'5550	9.29	+0.89	+1.09			+2.03	+2.60	+2.71	[+0.363	+0.069	+0.333]	6.38 ± 0.37
G24 - 3	10.46	+0.48	+0.30	+0.51	+0.82	+1.10	+1.43	+1.46	+0.371	+0.109	+0.210	
HD 193901	8.66	+0.55	+0.40			+1.14	+1.48	+1.52	[+0.288	+0.081	+0.367]	4.96 ± 0.52
G186 - 26	10.83	+0.40	+0.15	+0.45	+0.79	+0.95	+1.20	+1.23	[+0.384	+0.169	+0.431]	4.83 ± 0.27
HD 194598	8.35	+0.49	+0.30	+0.49	+0.84	+1.06	+1.35	+1.45	+0.371	+0.059	+0.319	1.01 ± 2.17
HD 197076	6.42	+0.62	+0.69	+0.49	+0.84	+1.06	+1.40	+1.44	+0.581	+0.299	+0.417	5.97 ± 0.30
BD + 4'4551	9.61	+0.51	+0.34	+0.69	+1.25	+1.12	+1.44	+1.49				
HD 199191	7.12	+0.96	+1.57	+0.56	+0.96	+1.73	+2.29	+2.34				
HD 199476	7.80	+0.69	+0.83	+0.56	+0.96	+1.26	+1.63	+1.69				

TABLE I. (continued)

Star	$V$	$B - V$	$U - V$	$V - R_J$	$V - I_J$	$V - J$	$V - H$	$V - K$	$b - y$	$m_1$	$c_1$	$M_0 (M_\odot)$
HD 199802	8.87	+0.57	+0.55	+0.50	+0.87	+1.16	+1.45	+1.51	+0.70	+0.24	-0.05	6.46 ± 0.66
HD 201626	8.14	+1.11	+1.60	+0.48	+0.81	+1.79	+2.30	+2.38	+0.348	+0.111	+0.261	5.43 ± 0.32
HD 201891	7.37	+0.51	+0.34	+0.54	+0.91	+1.095	+1.37	+1.42				4.57 ± 0.76
HD 201889	8.06	+0.59	+0.55	+0.51	+0.85	+1.21	+1.57	+1.61				
BD + 4°4674	8.50	+0.57	+0.52	+0.47	+0.79	+1.12	+1.47	+1.51	+0.309	+0.108	+0.439	3.47 ± 0.33
HD 207978	5.51	+0.42	+0.30	+0.38	+0.79	+0.88	+1.13	+1.17	+0.336	+0.131	+0.288	3.95 ± 0.43
HD 208906	6.96	+0.50	+0.38	+0.47	+0.79	+1.04	+1.31	+1.35				
HD 210295	9.57	+0.89	+1.30	+0.455	+0.795	+1.73	+2.30	+2.38				
BD + 17°4708	9.465	+0.44	+0.24	+0.455	+0.795	+1.055	+1.345	+1.395	+0.325	+0.069	+0.338	5.35 ± 1.01
BD + 7°4841	10.37	+0.46	+0.30			+1.03	+1.35	+1.39	[+0.344	+0.080	+0.352]	
BD + 39°4926	9.24	+0.21	+0.33	+0.54	+0.92	+0.68	+0.87	+0.94	+0.173	+0.036	+1.601	6.23 ± 0.30
HD 216777	8.01	+0.63	+0.71	+0.55	+0.93	+1.24	+1.56	+1.60	+0.400	+0.196	+0.275	5.39 ± 0.40
HD 218209	7.49	+0.645	+0.705			+1.25	+1.57	+1.62				
BD - 0°4470	9.95	+0.70	+0.705			+1.47	+1.93	+2.01	+0.463	+0.207	+0.110	
BD + 38°4955	11.04	+0.65	+0.50	+0.65	+1.11	+1.44	+1.86	+1.93	+0.473	+0.072	+0.097	9.62 ± 0.54
HD 219617	8.16	+0.48	+0.28	+0.45	+0.78	+1.07	+1.355	+1.39	+0.342	+0.086	+0.214	5.15 ± 0.52
BD + 2°4651	10.22	+0.43	+0.22			+1.05	+1.33	+1.37	[+0.341	+0.064	+0.406]	
BD + 59°2723	10.47	+0.44	+0.22			+1.08	+1.39	+1.42	+0.356	+0.058	+0.280	
HD 221170	7.70	+1.08	+1.64			+2.11	+2.73	+2.85	+0.737	+0.020	+0.603	
HD 221950	5.69	+0.44	+0.34	+0.42	+0.72	+0.89	+1.16	+1.19	+0.305	+0.120	+0.394	
HD 222589	8.74	+0.78	+1.18	+0.66	+1.12	+1.46	+1.91	+1.96	+0.428	+0.189	+0.215	4.76 ± 1.49
HD 224930	5.75	+0.665	+0.715	+0.61	+1.05	+1.415	+1.80	+1.88				5.29 ± 0.08
HD 225239	6.10	+0.63	+0.70	+0.55	+0.94	+1.27	+1.61	+1.67				3.76 ± 0.38

Note to Table I

 $(b - y)$ ,  $m_1$ , and  $c_1$  values within brackets refer to  $B - Y$ ,  $M_1$ , and  $C_1$  data of Eggen (1978).

to be double, although this is doubted by Eggen (1979). Several wide common proper motion pairs exist among the halo population: G89 – 13,14 (separation about 6'), the latter of which is one of Sandage's suggested binaries; G112 – 43,44 (separation 12"); and the well-known pair HD 134439,40 (separation about 5').

The purpose of this paper is to use photometric means to survey a larger number of halo stars that have been heretofore systematically studied. Our goal is to identify new binary candidates as well as estimate the binary frequency.

## II. THE METHOD

In a recent study of Hyades dwarfs, Carney (1982; hereafter referred to as Paper I) searched for binaries using *UBVRIJHK* photometry. At any fixed *V* – *K* color, stars with abnormally bright *V* or *K* magnitudes were identified as binaries with similar components, while stars with abnormal *B* – *V* colors were suggested to be binaries with dissimilar components. The magnitude excess method cannot be applied to field stars with uncertain relative distances, but of the 11 known and the 22 total known and suggested binaries in the Hyades, half were detected by the *B* – *V* color excess technique. We will apply here a similar method to the halo dwarfs. Before we begin comparing blue and red colors, how-

ever, we must overcome several additional barriers that arise when we restrict ourselves to a miscellaneous sample of field stars. First, we must select for study only halo stars. Second, we must weed out stars in a post-main-sequence stage of evolution. Such stars will be much brighter than a typical main-sequence companion and consequently completely dominate the flux distribution except in special cases. Third, we must rely on colors that have as little metallicity sensitivity as possible. In a cluster one may generally assume unique color-color relations for single stars because all stars have the same composition and only temperature is a variable. In the field, the variety of compositions forces us to be more selective. We will take up each of these problems in turn, then look for binaries based on a carefully selected sample of halo dwarfs based on metallicity-insensitive blue and infrared colors.

## III. ANALYSIS

### a) The Data

In Table I we list *UBVRIJHK* and *uvby* photometric data for 186 stars, representing most of the field stars whose *JHK* magnitudes have been determined by Carney and Aaronson (1979; hereafter referred to as CA) and Paper I. The remaining data have been taken from many sources, including Carney (1978a, b, 1980, 1983),

TABLE II. Single Hyades dwarfs photometry.

<i>vA/vB</i> *	<i>V</i>	<i>B</i> – <i>V</i>	<i>U</i> – <i>V</i>	<i>V</i> – <i>R<sub>J</sub></i>	<i>V</i> – <i>I<sub>J</sub></i>	<i>V</i> – <i>J</i>	<i>V</i> – <i>H</i>	<i>V</i> – <i>K</i>	<i>b</i> – <i>y</i>	<i>m</i> <sub>1</sub>	<i>c</i> <sub>1</sub>
17*	8.46	+0.70	+0.94	+0.545	+0.935	+1.28	+1.57	+1.64			
60	8.06	+0.64	+0.81	+0.535	+0.875	+1.19	+1.45	+1.50			
72	11.56	+1.375	+2.665			+2.66	+3.25	+3.39			
79	6.32	+0.40	+0.42	+0.375	+0.595	+0.77	+0.92	+0.95	+0.259	+0.175	+0.524
146	12.00	+1.41				+2.89	+3.55	+3.70			
156	8.46	+0.72	+1.03	+0.585	+0.965	+1.26	+1.585	+1.645	+0.440	+0.270	+0.331
215	6.61	+0.41	+0.41	+0.375	+0.615	+0.79	+0.95	+0.97	+0.267	+0.167	+0.482
276	10.51	+1.23				+2.34	+2.89	+3.01			
294	10.90	+1.29	+2.59			+2.44	+3.00	+3.13			
301	4.80	+0.16	+0.28	+0.155	+0.235	+0.33	+0.37	+0.38	+0.081	+0.210	+0.981
49*	8.24	+0.59	+0.71	+0.505	+0.825	+1.13	+1.38	+1.42			
310	9.98	+1.04	+1.99	+0.835	+1.395	+1.87	+2.35	+2.43			
315	6.97	+0.44	+0.44	+0.415	+0.685	+0.86	+1.04	+1.07	+0.294	+0.164	+0.458
319	7.80	+0.60	+0.73	+0.515	+0.865	+1.14	+1.435	+1.48	+0.384	+0.204	+0.328
354	11.18	+1.31				+2.49	+3.09	+3.20			
384	7.49	+0.54	+0.62	+0.48	+0.78	+1.035	+1.29	+1.34	+0.349	+0.187	+0.365
400	8.12	+0.66	+0.86	+0.555	+0.895	+1.19	+1.49	+1.54	+0.411	+0.226	+0.352
407	10.48	+1.14	+2.16			+2.09	+2.60	+2.72			
435	10.41	+1.09	+2.05			+2.07	+2.56	+2.67			
446	7.42	+0.54	+0.60	+0.47	+0.75	+1.01	+1.24	+1.27	+0.347	+0.176	+0.378
459	9.48	+0.93	+1.63			+1.62	+2.025	+2.115			
495	7.85	+0.61	+0.74	+0.505	+0.805	+1.10	+1.375	+1.425	+0.382	+0.207	+0.355
502	12.00	+1.41				+2.94	+3.60	+3.73			
544	6.92	+0.45	+0.45	+0.42	+0.67	+0.89	+1.07	+1.11	+0.300	+0.162	+0.436
547	8.96	+0.83	+1.32	+0.65	+1.07	+1.45	+1.815	+1.88	+0.497	+0.341	+0.315
548	10.32	+1.15	+2.23	+1.005	+1.655	+2.14	+2.65	+2.77			
560	9.09	+0.86	+1.44	+0.665	+1.115	+1.50	+1.87	+1.93			
589	5.48	+0.26	+0.36	+0.235	+0.365	+0.46	+0.53	+0.53	+0.142	+0.233	+0.795
591	5.40	+0.26	+0.35	+0.245	+0.405	+0.52	+0.62	+0.65	+0.154	+0.201	+0.814
622	11.94	+1.44				+2.92	+3.59	+3.74			
625	7.78	+0.54	+0.60	+0.475	+0.775	+1.03	+1.25	+1.29	+0.342	+0.194	+0.366
645	11.02	+1.29	+2.55			+2.405	+2.985	+3.10			
692	8.66	+0.74	+1.08	+0.605	+0.985	+1.30	+1.63	+1.70			
712	9.40	+0.88	+1.50	+0.695	+1.145	+1.54	+1.95	+2.02			
747	9.69	+0.91	+1.59	+0.745	+1.225	+1.61	+2.04	+2.12			
748	7.94	+0.63	+0.78	+0.545	+0.865	+1.145	+1.415	+1.46			
778	9.38	+0.85	+1.45	+0.675	+1.115	+1.52	+1.91	+1.98			

Sandage (1964, 1969), and Eggen (1978), as well as the homogeneous *UBV* catalog of Nicolet (1978) and the similar *uvby* catalog of Hauck and Mermilliod (1979). The *RI* data are all on the Johnson system, and the *JHK* data were taken in or transformed to the "CIT" system (see Paper II; Frogel *et al.* 1978; Elias *et al.* 1982). The *uvby* data come in two types: those in the standard system and those in a modified version (Eggen 1976, 1978).  $b - y$  colors are identical in both systems, but there are slight differences in the  $m_1$  index and large differences in the  $c_1$  index. We cannot overlook the large amount of data gathered by Eggen, and we will refer to his colors as  $B - Y$ ,  $M_1$ , and  $C_1$ , following his suggestion. In Table I such data are enclosed in brackets. We also include in Table I the absolute magnitudes derived from trigonometric parallaxes, without corrections for any of the usual systematic errors (Lutz and Kelker 1973; Hanson 1979).

In Table II we summarize equivalent photometric data for the 37 Hyades dwarfs that, according to Paper I, do not show either a magnitude or a color excess. These stars will serve as a homogeneous-composition sample of single dwarfs.

### b) Program Star Selection

#### 1) Metallicity

Table I contains a wide variety of halo stars: dwarfs, blue stragglers, subgiants, red giants, and horizontal branch stars. The stars also have a wide spread in metallicity, for although most have  $[\text{Fe}/\text{H}] < -1$ , there are a few solar-metallicity interlopers. We wish to restrict our sample to only the most metal-poor stars, which are presumably the oldest stars and which formed during the envisioned protogalactic collapse. A restriction to the lowest metallicities will also effectively reduce the metallicity sensitivity of many of the colors since the line blanketing will be severely diminished.

We make a first cut of the stars by setting a metallicity limit of  $[\text{Fe}/\text{H}] \leq -1.3$ . For most stars a spectroscopic abundance analysis has not been performed, and so we will usually work with a photometric ultraviolet excess. We have two such quantities generally available:  $\delta(U-B)_{0.6}$  (Sandage 1969; Carney 1979a) and  $\Delta m_1^*$ . The latter is defined to be

$$\Delta m_1^* = g[m_1(\text{star}) - m_1(\text{Hyades})],$$

where the  $m_1$  values are compared at equal  $b - y$  colors.  $g$  is the "guillotine," which normalizes the change in  $m_1$  to fixed changes in metallicity and is a function of temperature. According to the synthetic colors of Kurucz (1979, 1980) and CA,

$$g \sim 6.78 - 23.45(b - y) + 22.5(b - y)^2, \quad (2)$$

valid for  $0^m3 \leq (b - y) \leq 0^m55$ . According to Carney (1979a), the limiting  $[\text{Fe}/\text{H}]$  of  $-1.3$  corresponds to  $\delta(U-B)_{0.6} \geq 0^m20$ . A plot of  $\Delta m_1^*$  vs  $\delta(U-B)_{0.6}$  (Fig. 1) indicates this in turn means  $\Delta m_1^* \geq 0^m11$ . To minimize

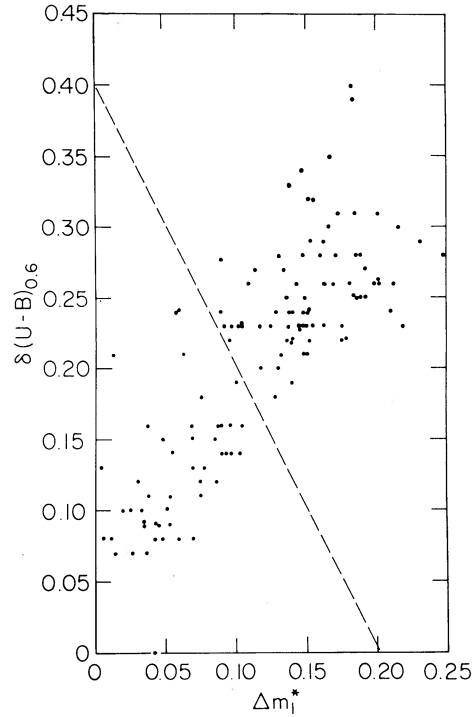


FIG. 1. The two ultraviolet excess metallicity indicators  $\delta(U-B)_{0.6}$  and  $\Delta m_1^*$  are plotted against each other. The diagonal line represents the metallicity cutoff of criterion 1 in the text.

the effects of photometric errors, we accept only those stars that meet one or more of the following criteria:

1. spectroscopic abundance analysis  $[\text{Fe}/\text{H}] \leq -1.3$ ;
2.  $\delta(U-B)_{0.6} + 2\Delta m_1^* \geq 0^m40$ ;
3.  $\delta(U-B)_{0.6} \geq 0^m25$ ; or
4.  $\Delta m_1^* \geq 0^m15$ .

As a result of this filtering, we obtain a preliminary sample of 87 program stars. Notice that the color restrictions introduced by the above criteria,  $0^m35 \leq (B - V) \leq 0^m90$  and  $0^m30 \leq (b - y) \leq 0^m55$ , effectively remove many of the blue stragglers, red giants, and horizontal branch stars.

#### 2) Gravity

To eliminate the intrinsically brighter post-main-sequence stars from our sample, we rely on three basic methods: parallaxes, spectroscopy, and photometry. In Table III we list the 87 metal-poor stars selected via the above metallicity criteria, their spectroscopic abundances where available, their ultraviolet excesses, and the results of the three tests: (blank) where no data are available, (0) for an indeterminate result, and (−) and (+) for rejection and acceptance, respectively.

The first test is that of the trigonometric parallax, using the data given in Table I. Several stars have excellent parallax data, and they have been used to define the

TABLE III. Gravity tests for metal-poor stars.

Star	$\delta(U-B)_{0.6}$	$\Delta m_{\text{r}}^{\dagger}$	$\pi$	spec. g	$c_1$	$G$	[Fe/H]	Comments
HD 3567	0.18	0.128	0	0	+			
BD + 71 <sup>o</sup> 31	0.24	0.210	+	0	+:			
HD 6755	0.23	0.147	0	-	-		-1.4	subgiant
HD 7424	0.31	0.077?	0	0	- , +			$c_1$ uncertain
BD + 72 <sup>o</sup> 94	0.28	0.131	0	0	+			
BD + 29 <sup>o</sup> 366	0.20	0.118	0	0	+			
HD 16031	0.25	0.136	0	0	+	0		
BD + 9 <sup>o</sup> 352	0.29	0.152	0	0	+			
G4 - 37	0.25	0.189	0	0	+	+		
HD 19445	0.28	0.171	+	+	std		-1.9	
BD + 11 <sup>o</sup> 468	0.24	0.129	0	0	+			
BD + 66 <sup>o</sup> 268	0.32	0.153	+	0	+			
HD 21581	0.39	0.184	0	-	std			red giant
HD 25329	0.24	0.057	+	+	std		-1.3	
BD + 21 <sup>o</sup> 607	0.23	0.154	0	0	+	+		
BD + 3 <sup>o</sup> 740	0.28	0.160	0	0	+			
G102 - 47	0.23	0.124	0	0	+			
BD + 37 <sup>o</sup> 1458	0.24	0.148	0	0	+			
HD 45282	0.21	0.149	0	0	-			
G89 - 14	0.23	0.137	0	0	+			
BD + 19 <sup>o</sup> 1730	0.23	0.145	0	0	+			
G90 - 3	0.22	0.176	0	0	+			
BD + 24 <sup>o</sup> 1676	0.30	0.166	0	0	+			
HD 64090	0.27	0.116	+	+	std		-1.7	
BD + 80 <sup>o</sup> 245	0.22	0.137	0	0	+			
BD + 54 <sup>o</sup> 1216	0.23	0.144	0	0	+			
HD 74000	0.29	0.231	+	+	std		-2.0	
G115 - 22	0.23	0.101	0	0	+	+		
BD - 3 <sup>o</sup> 2525	0.24	0.138	0	0	+			
BD + 9 <sup>o</sup> 2190	0.26	0.199	0	0	+	+		
BD + 1 <sup>o</sup> 2341p	0.31	0.173	+:	+	std		-2.7	
HD 84937	0.28	0.186	+	+	std		-2.2	
BD + 44 <sup>o</sup> 1910	0.25	0.186	0	0	+:	-		reject
BD + 58 <sup>o</sup> 1218	0.23	0.219	0	-	std			red giant
HD 87140	0.24	0.140	0	0	-			
BD + 29 <sup>o</sup> 2091	0.29	0.162	+	0	+			
HD 94028	0.22	0.137	+:	+:	+	+	-1.7	
G10 - 4	0.34	0.147	+	0	+	-		accept
BD + 36 <sup>o</sup> 2165	0.25	0.149	0	0	+	+		
BD + 51 <sup>o</sup> 1696	0.23	0.117	0	0	+	0		
HD 103095	0.19	0.100	+	+	std		-1.3	binary
BD - 4 <sup>o</sup> 3208	0.26	0.212	0	0	+			
G11 - 44	0.26	0.201	+:	0	+	+		
HD 106038	0.21	0.150	+	0	+	+		
HD 108177	0.28	0.148	+	+	+		-1.7	
BD + 28 <sup>o</sup> 2137	0.30	0.216	0	0	+			
G60 - 48	0.26	0.143	0	0	+	0		
G64 - 12	0.31	0.201	0	+	std		-3.5	
BD + 34 <sup>o</sup> 2476	0.25	0.185	+	+	+		-2.3	
BD + 26 <sup>o</sup> 2606	0.28	0.249	0	0	+	+		
G66 - 30	0.22	0.095	0	0	+			
HD 132475	0.23	0.148	+	+	+:	-	-1.0	accept
HD 134439	0.23	0.097	+	+	std		-1.5	
HD 134440	0.28	0.090	+	+	std		-1.5	
G15 - 24	0.21	0.132	0	0	+	+		
HD 140283	0.26	0.181	+	+	std		-2.5	
BD - 16 <sup>o</sup> 4187	0.46	...	0	0	?			ext. dK?
BD + 42 <sup>o</sup> 2667	0.24	0.151	0	-:	+	+	-1.7	accept
G180 - 58	0.33	0.139	0	+	0	0		
BD - 6 <sup>o</sup> 4455	0.25	...	0	?				insuff. data
HD 149414	0.24	0.089	+	0	+		-1.3	binary
BD + 2 <sup>o</sup> 3375	0.27	0.192	0	0	+	+		
BD - 8 <sup>o</sup> 4501	0.23	0.175	0	0	0			insuff. data
HD 161770	0.25	0.191	0	0	-			
BD + 20 <sup>o</sup> 3603	0.22	0.177	0	+	+		-2.3	
G154 - 34	0.40	0.182	+:	0	+		-1.6	ext. dK?
HD 163810	0.20	0.129	+	0	+:			binary
BD + 13 <sup>o</sup> 3683	0.26	0.202	0	0	?	-		reject
G206 - 34	0.31	0.185	0	0	+	+		
HD 175305	0.23:	0.106:	0	-	std		-1.5	red giant
HD 181007	0.28	...	0	0				insuff. data
BD + 26 <sup>o</sup> 3578	0.28	0.188	0	-	+		-2.3	reject
HD 188510	0.26	0.109:	0	0	+	+	-1.8	
G24 - 3	0.22	0.152	0	0	+			

TABLE III. (continued)

Star	$\delta(U-B)_{0.6}$	$\Delta m^*$	$\pi$	spec. g	$c_1$	$G$	[Fe/H]	Comments
HD 193901	0.23	0.104	+	0	+	0		
G186 - 26	0.32	0.155	0	0	+			
HD 194598	0.22	0.138	+	0	+	+		
BD + 4°4551	0.23	0.162	0	0	+			variable?
HD 201891	0.23	0.104	+	+	std		-1.4	
HD 210295	0.32		0	0				insuff. data
BD + 17°4708	0.24	0.152	0	+	+		-1.9	
BD + 7°4841	0.19	0.140	0	0	+			
BD - 0°4470	0.26	0.088	0	0	+			
BD + 38°4955	0.35	0.168	+	0	+			
HD 219617	0.27	0.134	+	0	+	+	-1.4	binary
BD + 2°4651	0.26	0.162	0	0	+			
BD + 59°2723	0.26	0.168	0	0	+			

standard halo dwarf sequence against which the other stars are tested (see Carney 1979b for a discussion of this locus).

Spectroscopic tests come in two forms. First, there are the low-resolution luminosity criteria which can separate dwarfs from red giants or horizontal branch stars. Second, spectroscopic gravities may be obtained from high-resolution spectra as part of abundance analyses. Both tests were employed where available.

The photometric test used here is the  $c_1$  (or  $C_1$ ) index. As discussed by Bond (1980), the  $c_1$  index remains sensitive to gravity to temperatures typical of K stars. To discriminate between dwarfs and post-main-sequence stars, we use two approaches. First, we employ the syn-

thetic colors of Kurucz (1979, 1980) and CA. The zero points have been set by forcing agreement between Procyon's observed colors and synthetic colors from a model atmosphere with  $T_{\text{eff}} = 6500$  K,  $\log g = 4.0$ , and  $[Z] = 0$ :  $(b-y) = (b-y)_{\text{syn}}$  and  $c_1 = (c_1)_{\text{syn}} + 0^m05$ . Figure 2 shows the resultant  $c_1$  vs  $(b-y)$  plane for a variety of temperatures and gravities with  $[Z] = 0$ . The arrows at points with  $T_{\text{eff}} = 5500, 6500$ , and  $7500$  K show the effects of decreasing  $[Z]$  from 0 to  $-2$ . The synthetic colors do not extend to cool enough temperatures for this project (due to unincluded molecular opacities), so an empirical approach was also adopted. We used observed colors for stars known (by parallaxes or spectroscopic means) to be dwarfs or post-main-sequence stars to calibrate the  $c_1$  and  $C_1$  vs  $(b-y)$  relations. Figures 3(a) and 3(b) show the distribution of dwarfs (+) and post-main-sequence stars ( $\blacktriangle$ ) in the  $c_1 - (b-y)$  plane. The extra data in Fig. 3(b) were taken from Bond (1980), whose photometry matches Eggen's system if  $0^m084$  is added to Bond's  $c_1$  index.

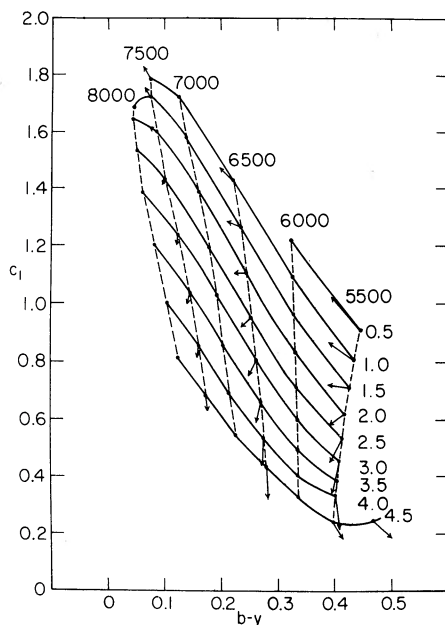


FIG. 2. Synthetic  $c_1$  indices and  $b-y$  colors for  $\log g = 0.5, 1.0, 1.5, 2.0, 2.5, 3.0, 3.5, 4.0$ , and  $4.5$ ;  $T_{\text{eff}} = 5000, 5500, 6000, 6500, 7000, 7500$ , and  $8000$  K; and  $[Z] = 0$ . A zero point shift was added to  $c_1$  to bring the synthetic colors for  $6500$  K,  $\log g = 4.0$ ,  $[Z] = 0$  into agreement with the observed  $c_1$  and  $b-y$  values for Procyon. The arrows represent the effects of decreasing  $[Z]$  from 0 to  $-2$ .

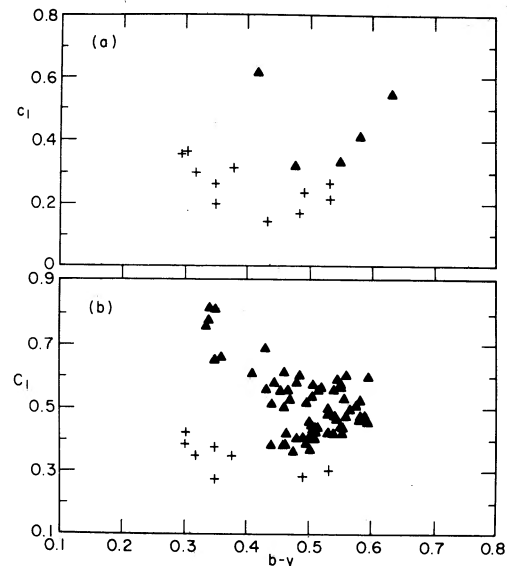


FIG. 3. (a) Empirical  $c_1$ ,  $(b-y)$  data for known halo dwarfs (+) and giants ( $\blacktriangle$ ); (b) same but for  $C_1$  vs  $B-Y$  (which equals  $b-y$ ).

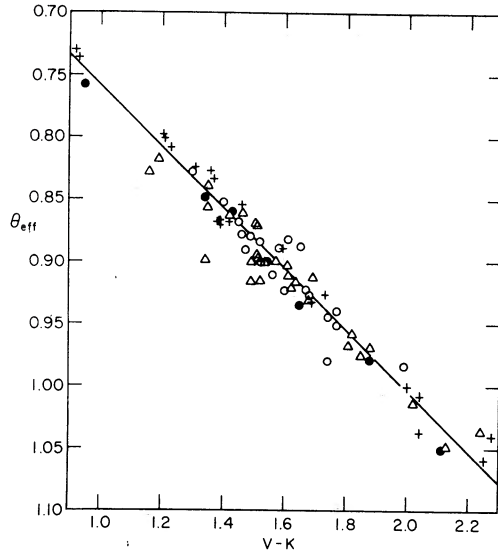


FIG. 4.  $\theta_{\text{eff}} (= 5040/T_{\text{eff}})$  vs  $V-K$  for the following classes of dwarfs: Hyades ( $\bullet$ );  $0^m0 < \delta(U-B)_{0.6} < 0^m1(0)$ ;  $0^m1 < \delta(U-B)_{0.6} < 0^m2(\Delta)$ ; and  $\delta(U-B)_{0.6} > 0^m2(+)$ . No metallicity sensitivity is apparent.

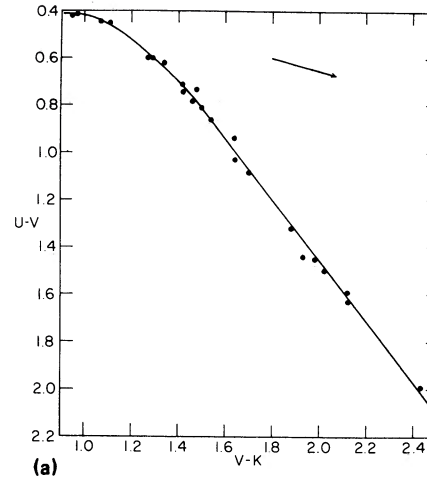
A supplemental photometric approach is available from the 13-color photometry of Schuster (1979). His system contains a gravity index "G," and we have employed the "control" stars discussed above to calibrate his data. Table III therefore also lists the results obtained from Schuster's photometry.

### c) Metallicity Sensitivity

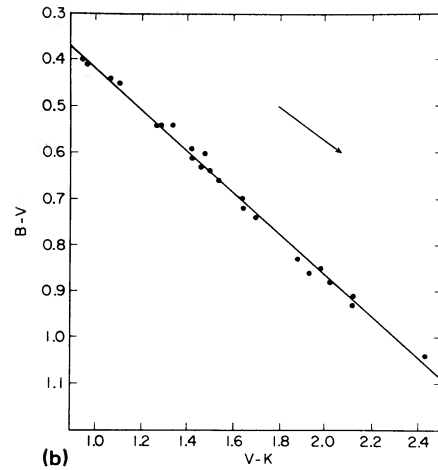
We will be best able to detect binaries with dissimilar components using blue versus infrared colors. To accurately establish the single-star color-color relation, we require little or no metallicity sensitivity in either color involved. We also prefer high photometric accuracy. From a consideration of the available data, we feel the best results will be obtained by comparing  $b-y$  to  $V-K$  colors.

To demonstrate the metallicity insensitivity of  $V-K$ , we show in Fig. 4 a plot for 78 stars of  $V-K$  vs  $\theta_{\text{eff}} (= 5040/T_{\text{eff}})$ . The temperatures were derived from comparisons of scanner spectrophotometric data given in Paper II with surface flux distributions of atomic line blanketed model atmospheres. Details were presented by Carney (1978a) and Peterson and Carney (1979) and are rediscussed in Appendix I. Metallicity differences have only a small effect on the surface fluxes, but were accounted for by using models computed with  $[Z] = 0, -1, \text{ and } -2$ . Figure 4 shows that for  $0.9 < V-K < 2.3$ ,  $V-K$  correlates with temperature without any perceptible metallicity sensitivity.

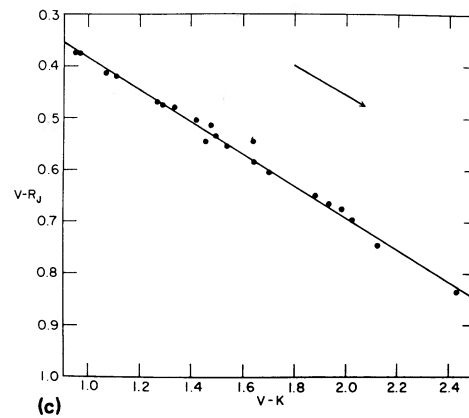
To investigate the metallicity sensitivities of the other possible colors, we could produce the requisite large number of such figures, but we choose for economy's sake to reproduce the approach of Johnson, MacArthur, and Mitchell (1968), who assumed  $R-I$  colors



(a)



(b)



(c)

FIG. 5.  $V-K$  vs other color indices for the single Hyades dwarfs of Paper I and Table II. Plotted against  $V-K$  are: (a)  $U-V$ ; (b)  $B-V$ ; (c)  $V-R_J$ ; (d)  $V-I_J$ ; (e)  $V-J$ ; (f)  $V-H$ ; (g)  $b-y$ . The arrows show the effects of  $E(B-V) = 0^m1$ .

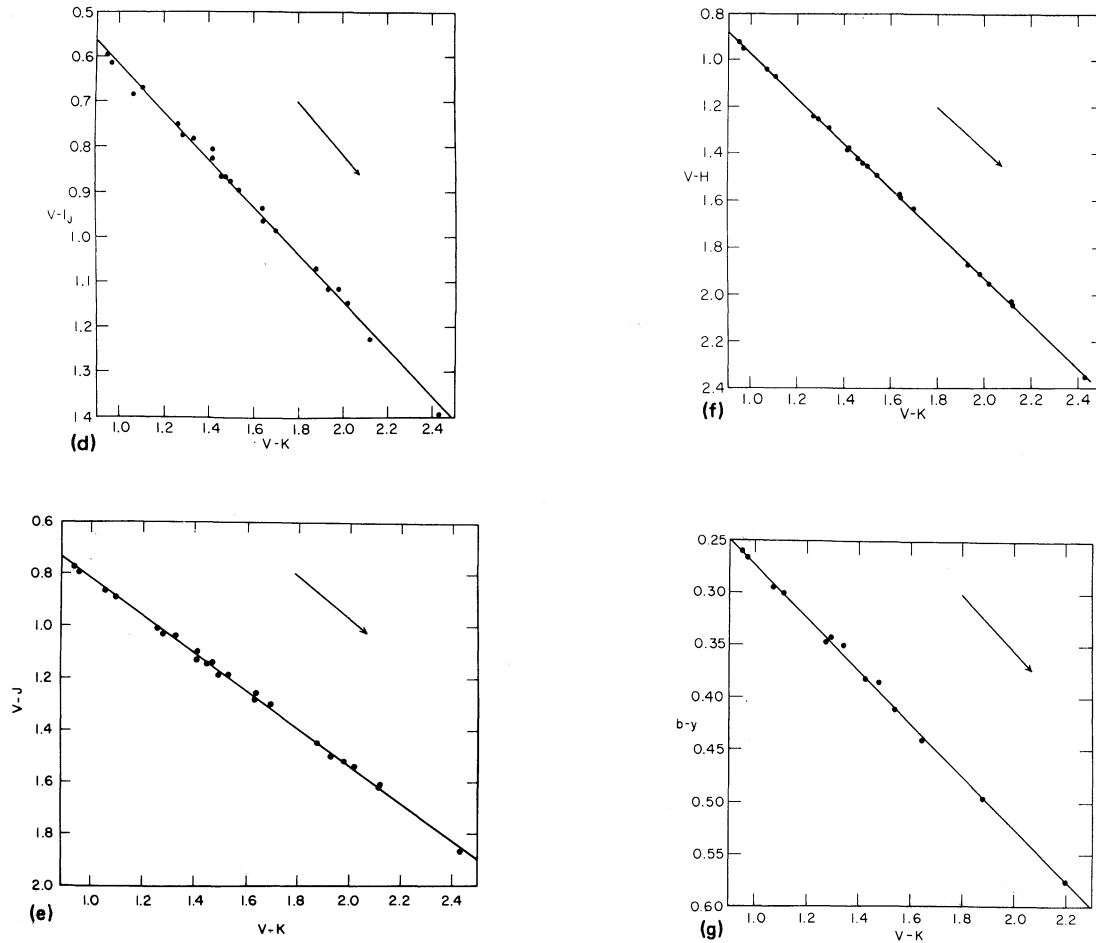


FIG. 5. (continued)

were independent of metallicity. They then compared colors of halo stars to those of Hyades dwarfs with equal  $R - I$  colors. The results showed approximately how the colors of metal-poor stars systematically differ from disk stars. We proceed similarly, except that we employ  $V - K$  as our metallicity-insensitive color and we use the 37 known single Hyades dwarfs of Table II. Figures 5(a)–(g) show the Hyades color-color relations. Except for the nonlinear  $U - V$  color, we find the following:

$$B - V = 0.454(V - K) - 0^m042, \quad (3a)$$

$$V - R_J = 0.308(V - K) + 0^m075, \quad (3b)$$

$$V - I_J = 0.529(V - K) + 0^m086, \quad (3c)$$

$$V - J = 0.730(V - K) + 0^m076, \quad (3d)$$

$$V - H = 0.957(V - K) + 0^m015, \quad (3e)$$

$$b - y = 0.253(V - K) + 0^m020. \quad (3f)$$

TABLE IV. Flux differences vs wavelengths.

Star	$V - K$	$\Delta(b - y)$	$\Delta(U - V)$	$\Delta(B - V)$	$\Delta(V - R)$	$\Delta(V - I)$	$\Delta(V - J)$	$\Delta(V - H)$
HD 3567	1.35	-0.032	-0.34	-0.111	-0.031	-0.010	-0.022	+0.014
BD + 71°31	1.34	-0.050	-0.44	-0.196			+0.016	+0.024
BD + 72°94	1.60	-0.116	-0.76	-0.304			+0.056	+0.005
BD + 29°366	1.55	-0.023	-0.385	-0.087	-0.032	+0.004	-0.028	+0.003
HD 16031	1.31	-0.028	-0.38	-0.113			-0.032	+0.003
BD + 9°352	1.415	-0.035	-0.53	-0.160			-0.024	-0.008
G4 - 37	1.415	-0.032	-0.46	-0.13			-0.014	+0.011
HD 19445	1.39	-0.023	-0.47	-0.129	-0.033	-0.001	-0.031	+0.006
BD + 11°468	1.59	-0.029	-0.54	-0.140			-0.017	+0.005
BD + 66°268	1.835	-0.042	-0.69	-0.131	-0.030	-0.017	-0.026	-0.009
HD 25329	2.275	-0.064	-0.585	-0.126	-0.026	-0.019	-0.026	-0.010

TABLE IV. (continued)

Star	$V-K$	$\Delta(b-y)$	$\Delta(U-V)$	$\Delta(B-V)$	$\Delta(V-R)$	$\Delta(V-I)$	$\Delta(V-J)$	$\Delta(V-H)$
BD + 21°607	1.325	-0.034	-0.38	-0.110	-0.023	+0.013	-0.033	-0.012
BD + 3°740	1.31	-0.044	-0.46	-0.193			-0.022	+0.008
G102 - 47	1.91	-0.056	-0.76	-0.185			-0.040	-0.001
BD + 37°1458	1.80	-0.047	-0.725	-0.180	-0.049	-0.028	-0.040	-0.006
G89 - 14	1.46	-0.066	-0.475	-0.156			-0.032	-0.001
BD + 19°1730	1.36	-0.033	-0.41	-0.135			-0.019	-0.005
G90 - 3	1.57	-0.041	-0.60	-0.191			-0.012	+0.014
BD + 24°1676	1.28	-0.046	-0.45	-0.179			0.000	+0.011
HD 64090	1.73	-0.027	-0.63	-0.133	-0.048	-0.031	-0.029	+0.001
BD + 80°245	1.79	-0.071	-0.86	-0.271			+0.007	+0.024
bD + 54°1216	1.335	-0.022	-0.35	-0.084	-0.061	-0.052	-0.011	+0.024
HD 74000	1.26	-0.022	-0.39	-0.110	-0.063	-0.062	-0.036	0.000
G115 - 22	1.61	-0.038	-0.49	-0.109			-0.021	+0.006
BD - 3°2525	1.495	-0.040	-0.53	-0.157	-0.035	-0.027	-0.027	-0.004
BD + 9°2190	1.27	-0.022	-0.40	-0.155			-0.028	+0.006
bD + 1°2341p	1.205	-0.030	-0.39	-0.145	-0.036	-0.043	-0.011	+0.008
HD 84937	1.21	-0.023	-0.36	-0.117	-0.058	-0.056	-0.029	-0.002
BD + 29°2091	1.50	-0.026	-0.54	-0.139			-0.021	+0.001
HD 94028	1.39	-0.029	-0.39	-0.109	-0.048	-0.036	-0.021	-0.004
G10 - 4	2.045	-0.029	-0.845	-0.166			-0.009	-0.015
BD + 36°2165	1.27	-0.027	-0.35	-0.105	-0.051	-0.018	-0.023	-0.004
BD + 51°1696	1.60	-0.033	-0.54	-0.134			-0.014	+0.015
HD 103095	2.02	-0.048	-0.605	-0.125	-0.042	-0.040	+0.009	+0.014
BD - 4°3208	1.31	-0.030	-0.42	-0.148			-0.012	+0.023
G11 - 44	1.37	-0.013	-0.46	-0.155			-0.016	+0.045
HD 106038	1.395	-0.027	-0.405	-0.121	-0.040	-0.019	-0.029	+0.006
HD 108177	1.32	-0.031	-0.435	-0.127	-0.027	-0.004	-0.030	+0.013
BD + 28°2137	1.35	-0.037	-0.49	-0.171			-0.042	+0.024
G60 - 48	1.47	-0.038	-0.51	-0.145			-0.019	0.000
G64 - 12	1.22	-0.028	-0.39	-0.132	-0.046	-0.046	-0.037	+0.009
BD + 34°2476	1.23	-0.030	-0.36	-0.121	-0.034	-0.027	-0.024	+0.019
BD + 26°2606	1.37	-0.039	-0.475	-0.155	-0.047	-0.036	-0.016	+0.015
G66 - 30	1.26	-0.056	-0.34	-0.130			-0.016	0.000
HD 132475	1.625	-0.045	-0.55	-0.141	-0.051	-0.041	-0.027	+0.016
HD 134439	2.04	-0.046	-0.60	-0.124	-0.013	-0.015	-0.005	+0.025
HD 134440	2.25	-0.058	-0.56	-0.116	+0.006	+0.015	-0.009	+0.014
G15 - 24	1.63	-0.021	-0.52	-0.128			-0.056	+0.007
HD 140283	1.59	-0.045	-0.66	-0.200	-0.055	-0.057	+0.003	+0.025
BD + 42°2667	1.36	-0.026	-0.40	-0.115	-0.029	-0.005	-0.039	+0.005
G180 - 58	1.90	-0.035	-0.74	-0.141			-0.023	-0.001
HD 149414	2.09	-0.074	-0.74	-0.167	-0.019	-0.002	-0.042	+0.007
BD + 2°3375	1.46	-0.040	-0.56	-0.171	-0.045	-0.028	-0.022	+0.009
BD + 20°3603	1.20	-0.004	-0.265	-0.063	-0.115	-0.091	-0.062	-0.002
G154 - 34	1.76	+0.015	-0.59	-0.067			-0.031	+0.022
HD 163810	1.91	-0.075	-0.84	-0.225	-0.063	-0.086	-0.080	-0.011
G206 - 34	1.34	-0.017	-0.49	-0.166			-0.044	+0.024
HD 188510	1.69	-0.040	-0.59	-0.135	-0.026	-0.040	-0.030	+0.009
G24 - 3	1.46	-0.026	-0.47	-0.141			-0.042	+0.019
HD 193901	1.52	-0.034	-0.44	-0.098	-0.033	-0.070	-0.046	+0.012
G186 - 26	1.23	-0.043	-0.40	-0.116			-0.024	+0.009
HD 194598	1.38	-0.020	-0.38	-0.095	-0.050	-0.026	-0.023	+0.016
BD + 4°4551	1.49	-0.026	-0.45	-0.124			-0.044	-0.004
HD 201891	1.42	-0.031	-0.38	-0.093	-0.032	-0.027	-0.018	-0.003
BD + 17°4708	1.395	-0.048	-0.46	-0.151	-0.050	-0.029	-0.039	-0.004
BD + 7°4841	1.39	-0.028	-0.39	-0.129			-0.061	+0.006
BD - 0°4470	2.01	-0.066	-0.775	-0.171			-0.073	-0.007
BD + 38°4955	1.93	-0.035	-0.88	-0.184	-0.019	+0.003	-0.045	0.000
HD 219617	1.39	-0.030	-0.41	-0.109	-0.053	-0.041	-0.021	+0.011
BD + 2°4651	1.37	-0.026	-0.45	-0.150			-0.026	+0.005
BD + 59°2723	1.42	-0.023	-0.50	-0.163			-0.033	+0.017

We next compute the flux differences  $\Delta(\text{color}) = \text{color}(\text{halo dwarf}) - \text{color}(\text{Hyades})$  at equal  $V-K$ , and list the results in Table IV. If we average the results, we obtain Fig. 6, which confirms the earlier work of Johnson, MacArthur, and Mitchell (1968).  $U-V$ ,  $B-V$ , and  $U-B$  are obviously very metal sensitive, which of course forms the basis of our  $\delta(U-B)_{0.6}$  and  $\Delta m_1^*$  in-

dices. We also note, however, that  $V-R_j$  is sensitive to some degree. In fact, no other color is as satisfactory a temperature indicator as  $V-K$  over this temperature range. Its only observational drawback is that  $V$  and  $K$  are measured with different instruments on different nights, but that is offset by the long wavelength base line involved [note the slope of the  $\theta_{\text{eff}} - (V-K)$  relation in

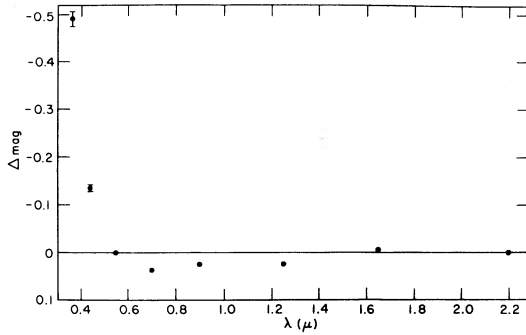


FIG. 6. The net average flux difference,  $\Delta(\text{color}) = V - \lambda$  (halo dwarf) -  $V - \lambda$  (Hyades dwarf) at equal  $V - K$ . The figure is the average of the stars in Table IV and shows how flux is redistributed as metal lines are removed from a stellar photosphere. Halo dwarfs are, for example, much brighter than Hyades dwarfs in the  $U$  bandpass but fainter in the  $R_J$  bandpass at equal effective temperatures.

#### Appendix I].

#### IV. RESULTS

In Fig. 7 we show the halo dwarf versus Hyades dwarf flux differences given in Table IV as a function of  $V - K$ . A linear least-squares fit is

$$\Delta(b - y) = -0.020(V - K) - 0^m004, \quad (4)$$

with  $\sigma = 0^m010$  if we remove the known binaries and the few stars that significantly deviate from the mean relation. The fact that  $\Delta(b - y) \neq 0^m000$  merely indicates that  $b - y$  is slightly metal sensitive, and Eq. (4) in turn shows the sensitivity is, not surprisingly, mildly dependent on temperature. We tentatively identify as binaries those stars that differ from the mean relation by  $3\sigma$  ( $0^m030$ ) or more. Since all the program halo stars are very metal poor, decreases in  $[\text{Fe}/\text{H}]$  from  $-1.3$  to  $-3.5$  (the total range involved), should not affect the colors by any detectable amount. Indeed, G64 - 12 ( $[\text{Fe}/\text{H}] = -3.5$ ; Carney and Peterson 1981a) falls exactly on the mean line. Instead, we attribute the scatter about the mean line to observational errors, estimated as  $\pm 0^m010$ , and the presence of binaries with dissimilar components. Note that according to the reddening vec-

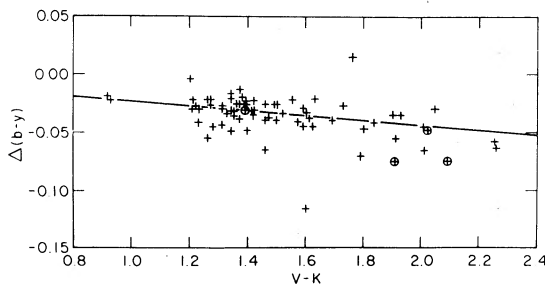


FIG. 7. The flux differences  $\Delta(b - y)$  for the stars of Table IV plotted against  $V - K$ . Circles enclose known binaries.

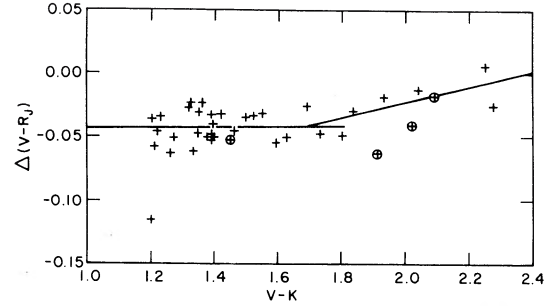


FIG. 8. Same as Fig. 7, but for  $\Delta(V - R_J)$ .

tors in Figs. 5(b)-(g), variable reddening will have no effect on the scatter. In Figs. 8 and 9, we repeat the procedure for  $\Delta(V - R_J)$  and  $\Delta(V - J)$ , respectively. Again we note G64 - 12 falls right at the mean. We choose not to use  $\Delta(V - I_J)$  because the scatter is too large, and  $\Delta(V - H)$  is not capable of detecting binaries generally because of the small wavelength differences involved between the  $H$  and  $K$  bandpasses. For the mean  $\Delta(V - R_J)$  relation we adopt

$$\Delta(V - R_J) = -0^m042 \text{ for } (V - K) \leq 1.7, \quad (5a)$$

$$\Delta(V - R_J)$$

$$= 0.061(V - K) - 0^m145 \text{ for } (V - K) > 1.7. \quad (5b)$$

$\Delta(V - J)$  has a constant value of  $-0^m026$ .  $\sigma[\Delta(V - R_J)] = 0^m012$ , and  $\sigma[\Delta(V - J)] = 0^m014$ .

In Table V we list the departure,  $\delta$ , of the colors of some halo stars from the mean relations of Figs. 7-9. We include only stars known to be binaries, suggested binaries based on this paper, and stars previously suggested to be binaries on the basis of suspected radial velocity variability. We take up these three classes of stars in turn.

#### a) Known Binaries

Four stars in Table V have visually and/or spectroscopically detectable companions. In two cases we do not expect to see any signs of the companions using our method: HD 103095's companion is very much fainter than the primary and so contributes little detectable ex-

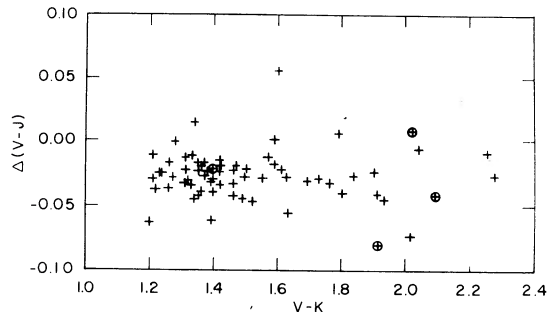


FIG. 9. Same as Fig. 7, but for  $\Delta(V - J)$ .

TABLE V. Halo binary candidates.

Star	$\delta\Delta (b - y)$	$\sigma$	$\delta\Delta (V - R_j)$	$\sigma$	$\delta\Delta (V - J)$	$\sigma$
(A) Known binaries						
HD 103095	-0.004	0.4	-0.020	1.7	+0.035	2.5
HD 149414	-0.029	2.9	-0.001	0.1	-0.016	1.1
HD 163810	-0.033	3.3	-0.035	2.9	-0.054	3.9
HD 219617	+0.002	0.2	-0.011	0.9	+0.005	0.4
(B) New candidates						
BD + 72°94	-0.080	8.0	...	...	+0.082	5.9
G89 - 14	-0.033	3.3	...	...	-0.006	0.4
BD + 80°245	-0.032	3.2	...	...	+0.033	2.4
BD + 20°3603	+0.024	2.4	-0.073	6.1	-0.036	2.6
G154 - 34	+0.054	5.4	...	...	-0.005	0.4
BD - 0°4470	-0.022	2.2	...	...	-0.047	3.4
(C) Suspected radial velocity variables						
HD 3567	-0.001	0.1	+0.011	0.9	+0.004	0.3
HD 16031	+0.002	0.2	...	...	-0.006	0.4
BD - 3°2525	-0.006	0.6	+0.007	0.6	-0.001	0.1
BD + 1°2341p	-0.002	0.2	+0.006	0.5	+0.015	1.1
HD 84937	+0.005	0.5	-0.016	1.3	-0.003	0.2
BD + 36°2165	+0.002	0.2	-0.009	0.8	+0.003	0.2
HD 132475	-0.008	0.8	-0.009	0.8	-0.001	0.1
G206 - 34	+0.014	1.4	...	...	-0.018	1.3
HD 188510	-0.002	0.2	+0.016	1.3	-0.004	0.3
BD + 38°4955	+0.008	0.8	+0.008	0.7	-0.019	1.4

cess flux at any wavelength; and HD 219617's companion is almost a twin to the primary, so the flux distribution is essentially unchanged. For HD 163810, however, the companion is known to be only about 1<sup>m</sup>3 fainter than the primary, and, indeed, is detectable using the  $\delta$  values for all three colors. The companion of HD 149414 has not yet been seen, although orbital motion is clearly present (Mayor and Turon 1982), but our  $\delta(b - y)$  result strongly suggests its presence. For HD 103095, we see some evidence for the companion using  $\Delta(V - J)$ , in spite of the large  $V$  magnitude difference between the primary and secondary ( $\sim 4^m5$ ). The method seems to work about half the time for the halo dwarfs, as it did for the Hyades dwarfs in Paper I.

#### b) New Candidates

Six new binary candidates are given in Table V, with four showing signs of a red companion, one (G154 - 34) signs of a blue companion, and one (BD + 20°3603) being indeterminate. The case for BD + 72°94 seems particularly strong, and unless the inclination is nearly zero, we expect the companion should be spectroscopically detectable. We note parenthetically that our photometric method is not affected by orbital inclination.

G89 - 14 has, as noted earlier, been identified by Sandage (1969) as a radial velocity variable suspect. G89 - 13, its proper motion companion, has a  $C_1$  index indicating it is a red giant. If so, G89 - 14 is too bright to be a single dwarf or subgiant, and a binary nature may help explain the anomalous brightness besides its unusual colors.

G154 - 34 is a particularly interesting case. It is a  $K$  dwarf but with an extreme ultraviolet excess, which Bessell and Wickramasinghe (1979) have argued is a sign that it may be one of the "missing" metal-poor  $K$  dwarfs. Wallerstein (1976) had previously pointed out the apparent lack of such cool stars with  $[\text{Fe}/\text{H}]$  values less than about -1.5, and had speculated that the effect might be real, due, perhaps, to the combination of extremely rapid nucleosynthesis during the formation of the galactic halo and the longer gravitational contraction time scale for lower mass stars. Bessell and Wickramasinghe, however, argued that such stars have simply been overlooked, and that the extreme ultraviolet excess  $K$  stars discussed by Eggen (1969) are the "missing" very low metallicity  $K$  dwarfs. G154 - 34 is one of the brighter of such stars, and our data indicate its ultraviolet excess may be due to a hot binary companion. Satellite ultraviolet data for this star and a few other members of this unusual class may shed light on whether the very low metallicity  $K$  dwarfs will remain missing.

The other two stars, BD + 80°245 and BD - 0°4470, appear to be normal halo dwarfs, but the photometry suggests faint red companions. Radial velocity surveys should be undertaken.

#### c) Previously Suggested Binary Candidates

Variable radial velocities have been reported for ten of the stars in Table IV, in addition to the four known binaries. Our photometric method does not show any signs of a companion for these stars, although such systems might resemble HD 103095 with an extremely

faint companion or HD 219617 with a twin. Not all ten stars are likely to be binaries, however.

Sandage (1964, 1969) has reported suspected radial velocity variability for HD 3567, BD - 3°2525, and HD 188510. Popper (1942) reported a radial velocity amplitude of about  $40 \text{ km s}^{-1}$  for BD + 36°2165 (Eggen 1964 incorrectly identified this star as BDS 5699, which is a much brighter pair lying about 5' NNW).

Eggen (1964) has also mentioned radial velocity variability for HD 16031, G206 - 34, and BD + 38°4955, although in the latter two cases Popper (1942) makes no such note. For HD 16031, Buscombe and Morris (1958) likewise do not mention such variability, so for all three stars we must consider the radial velocity variability as tentative and recommend further study.

Three of the ten stars are almost certainly not radial velocity variables. BD + 1°2341p has often been considered to be such a variable due to Popper's (1942) mistakenly observing BD + 1°2341f, then (Popper 1943) BD + 1°2341p. He noted the error in a footnote which has regrettably often been overlooked. We note the radial velocities obtained by Carney and Peterson (1981b) are in near-perfect agreement with Popper's proper value. Abt and Levy (1969) suggested HD 84937 is a probable variable with a period of about 7600 days, but this was not confirmed by the further study of the star by Crampton and Hartwick (1972). Finally, Alden (1938) claimed his parallax plates of HD 132475 indicated the presence of a binary with an orbital period of about 1300 days, which should result in a radial velocity amplitude of about  $12 \text{ km s}^{-1}$ . Popper (1942) reported such a variation, but considered the low quality of the spectrograms warranted more data. He later (Popper 1943) retracted his claim, and instead argued that no velocity variations greater than  $5 \text{ km s}^{-1}$  are present. HD 132475 is thus also not likely to be a binary.

#### d) Blue Stragglers

Carney and Peterson (1981b) have discussed the two well-known field halo blue stragglers, BD + 25°1981 and BD - 12°2669. The spectroscopic abundance analyses did not yield any unusual chemical abundance patterns indicative of mass transfer or mixing that might explain the blue straggler phenomenon, but the radial velocities are variable so mass transfer remains a possibility. A test of mixing versus mass transfer is to discover the evolutionary status of the companion, for if mass transfer has occurred, it should be a white dwarf. If the companion is an unevolved red dwarf, mass transfer has almost certainly not occurred. Regrettably, the photometric data presented here fail to reveal a companion for either star. Rejecting the similar components possibility since that would require two blue stragglers instead of one, and since both stars are single-lined spectroscopic binaries, we infer both companions are much fainter than the primaries. Given two such faint companions, we speculate that they are white dwarfs and that ultraviolet data will be required to detect them.

#### e) Halo Binary Frequency

Eight of the 71 stars in Table IV show photometric evidence for companions. Two are known binaries, and another is a suspected radial velocity variable. The photometric method of course cannot detect systems with similar components nor those with extremely faint companions. In Paper I the color excess method detected about half the known and suggested binaries, and this fraction appears to be roughly the same for the halo dwarfs. We therefore tentatively suggest that as many as 15 or 16 of the 71 stars are binaries, for a frequency of between 20% and 25%. Although this fraction is less than that of the disk population (> 50%), it is not zero, and we have cause to hope that a double-lined eclipsing halo population binary may yet be discovered.

#### V. SUMMARY

We have presented a list of 186 field stars for which *JHK* photometric data have been obtained over the past few years. From this sample we selected a subset of stars with a limited range in color and spectroscopic abundances or ultraviolet excesses indicative of  $[\text{Fe}/\text{H}] \leq -1.3$ . Use of parallax, spectroscopic, and photometric data then eliminated the post-main-sequence stars, leaving a total sample of 71 metal-poor halo stars. Comparisons of such stars with the 37 single Hyades dwarfs identified in Paper I yielded the metallicity sensitivities of various color indices. Comparisons of short and long wavelength colors, especially  $b - y$  vs  $V - K$ , of the halo dwarfs then revealed several stars with unusual flux distributions, presumably due to binary companions of differing spectral types. Two of the four known binaries and one of the seven suspected radial velocity variables were detected in this manner, as well as five new candidates. If the flux distribution method is as effective among the halo stars as it was in the Hyades (~50%), we estimate the halo dwarf binary frequency to be about 20%–25%.

I thank Dick Joyce of Kitt Peak for his instructions on the use of the KPNO infrared system. This research has been supported by NSF Grant AST 8111938.

#### APPENDIX I: EFFECTIVE TEMPERATURES

Peterson and Carney (1979) have discussed the effective temperature scale of dwarfs, based on comparisons of the spectrophotometry presented in Paper II with surface fluxes computed using R. L. Kurucz's model atmosphere program ATLAS6. Table 4 of the paper gives effective temperatures for 74 stars. New data require the following revisions: HD 87140 ( $\theta_{\text{eff}}$  changed from 1.002 to 1.000); HD 103095 ( $\theta_{\text{eff}}$  changed from 1.014 to 1.010); and HD 123710 ( $\theta_{\text{eff}}$  changed from 0.916 to 0.908). New temperatures for 13 stars, based on the 1979 KPNO spectrophotometry of Paper II, are given in Table VI.

TABLE VI. New effective temperatures.

Star	$\theta_{\text{eff}}$	$T_{\text{eff}}$	[Fe/H]	Comments
vA 79	0.757	6660		Hyades member
BD + 25°1981	0.736	6850	-1.5	halo blue straggler
BD - 12°2669	0.730	6900	-1.4	halo blue straggler
BD + 1°2341p	0.797	6325	-2.7	
HD 100363	0.715	7050	-0.3	low-amp. var. (SU Crt)
BD - 4°3208	0.824	6120		
HD 114095	1.113	4530		
BD + 34°2476	0.808	6240	-2.3	
HD 128167	0.757	6660	-0.6	data from Böhm-Vitense and Johnson (1979)
BD + 26°2606	0.833	6050		
BD + 42°2667	0.826	6100	-1.7	
BD + 2°3375	0.854	5900		
HD 185395	0.757	6660		data from Böhm-Vitense and Johnson (1979)

Figure 4 shows  $\theta_{\text{eff}}$  vs  $V-K$  for dwarfs of widely differing metallicity, demonstrating the metallicity insensitivity of  $V-K$ . The linear relation, valid from  $T_{\text{eff}} \sim 4500$  to 7000 K, is

$$\theta_{\text{eff}} = 0.245(V-K) + 0.514. \quad (\text{I-1})$$

As may be seen in Fig. 6, most other colors depend to some degree on metallicity, and some possible colors, such as  $R_J - J$ , are measured with different instruments on different nights and hence are prone to larger observational errors. We recommend use of  $b-y$  and  $(R-I)_J$  colors in addition to  $V-K$ .

For  $\delta(U-B)_{0.6} \geq 0^m20$  ( $[\text{Fe}/\text{H}] \leq -1.3$ ):

$$\theta_{\text{eff}} = 1.034(R-I)_J + 0.516, \quad (\text{I-2a})$$

$$\theta_{\text{eff}} = 1.093(b-y) + 0.479. \quad (\text{I-2b})$$

For  $\delta(U-B)_{0.6} \leq 0^m10$  ( $[\text{Fe}/\text{H}] \geq -0.4$ ):

$$\theta_{\text{eff}} = 0.999(R-I)_J + 0.544, \quad (\text{I-3a})$$

$$\theta_{\text{eff}} = 0.990(b-y) + 0.503. \quad (\text{I-3b})$$

For cases where the metallicity is unknown:

$$\theta_{\text{eff}} = 0.993(R-I)_J + 0.539, \quad (\text{I-4a})$$

$$\theta_{\text{eff}} = 1.069(b-y) + 0.483. \quad (\text{I-4b})$$

As a check on the technique, we here compute the temperature of Procyon, whose empirical effective temperature (Code *et al.* 1976) is  $6510 \pm 130$  K. The observed colors of Procyon are  $(V-K)_{\text{CIT}} = 1^m00$ ,  $(R-I)_J = 0^m23$  (Johnson *et al.* 1966), and

$(b-y) = 0^m272$  (Hauck and Mermilliod 1979). Using the  $\delta(U-B)_{0.6} \leq 0^m10$  relations, we obtain  $T_{\text{eff}} = 6560 \pm 40$ , whereas for the general relations,  $T_{\text{eff}} = 6575 \pm 40$ . The temperature scale might be too high by 50 K, but the errors are well within the observational uncertainties. In any event, these temperatures are the ones to use in high-resolution spectroscopic abundance analyses when ATLAS6 model atmospheres are employed.

#### APPENDIX II: BOLOMETRIC CORRECTIONS

Carney and Aaronson (1979) obtained empirical bolometric corrections for dwarfs with differing temperatures and metallicities by integrating over the *UBV-RIJHK* photometry, correcting for ultraviolet and far-infrared flux by model atmospheres, and comparing the results directly to a standard G2 V star. The substantial increase in *JHK* data, especially for halo and Hyades dwarfs (Papers I and II), warrants a second look. In Table VII we present new results for 70 additional stars, following the same procedures discussed by CA. We include  $\theta_{\text{eff}}$  values from the scanner spectrophotometry, as well as  $b-y$ ,  $(R-I)_J$ , and  $V-K$  colors where available, as well as the straight average. Table VI of CA should have the following additions for  $T_{\text{eff}} = 7000$  K:

[Z]	$F_{0-0.36}/F_{0-\infty}$	$F_{2.2-\infty}/F_{0-\infty}$
0	0.135	0.028
-1	0.184	0.028
-2	0.217	0.028

TABLE VII. Bolometric corrections.

Star	[Fe/H] <sup>a</sup>	B.C.	$T_{\text{eff}}$	$\theta_{\text{eff}}(\text{scan})$	$\theta_{\text{eff}}(b-y)$	$\theta_{\text{eff}}(R-I)$	$\theta_{\text{eff}}(V-K)$
HD 3567	(-1.0)	-0.19	5950	0.839	0.836	0.867	0.845
HD 4307	(-0.2)	-0.14	5650	0.900	0.886	0.894	0.886
BD + 29°366	(-1.2)	-0.20	5560		0.904	0.919	0.894
HD 13403	(-0.2)	-0.17	5500	0.913	0.905	0.934	0.913
BD - 1°306	(-1.0)	-0.19	5590	0.916	0.886	0.916	0.886
HD 13783	(-0.6)	-0.185	5480			0.916	0.923
BD + 66°268	(-2.7)	-0.27	5240		0.962	0.961	0.964
BD + 21°607	(-1.5)	-0.205	5960		0.830	0.868	0.839
HD 250792	(-1.0)	-0.245	5270			0.956	0.955

TABLE VII. (continued)

Star	[Fe/H] <sup>a</sup>	B.C.	$T_{\text{eff}}$	$\theta_{\text{eff}}(\text{scan})$	$\theta_{\text{eff}}(b-y)$	$\theta_{\text{eff}}(R-I)$	$\theta_{\text{eff}}(V-K)$
BD + 37 <sup>o</sup> 1458	(-1.7)	-0.26	5250		0.947	0.961	0.955
HD 45282	(-1.3)	-0.26	5160		0.977	0.971	0.981
HD 68017	(-0.4)	-0.16	5510	0.926	0.926	0.882	0.926
BD + 54 <sup>o</sup> 1216	(-1.5)	-0.185	5980		0.846	0.842	0.841
HD 70958	(-0.2)	-0.115	6190		0.811	0.824	0.808
HD 74000	-2.0	-0.205	6140		0.825	0.816	0.823
BD + 25 <sup>o</sup> 1981	-1.4	-0.20	6880	0.736	0.734	0.718	0.742
BD - 12 <sup>o</sup> 2669	-1.5	-0.205	6900	0.730	0.735	0.718	0.739
BD - 3 <sup>o</sup> 2525	(-1.7)	-0.23	5750		0.870	0.878	0.880
HD 80218	(-0.2)	-0.135	6050	0.828	0.838	0.834	0.832
BD + 1 <sup>o</sup> 2341p	-2.7	-0.23	6290	0.797	0.801	0.795	0.809
HD 87140	(-1.7)	-0.29	5010	1.000	1.004	1.012	1.004
BD + 36 <sup>o</sup> 2165	(-1.8)	-0.20	6050		0.822	0.852	0.825
HD 97916	-1.2	-0.185	6190		0.799	0.837	0.808
HD 106038	(-1.3)	-0.20	5860		0.857	0.868	0.856
HD 106516	-0.7	-0.15	6110		0.822	0.832	0.819
HD 108177	-1.7	-0.22	6000		0.832	0.852	0.837
HD 108754	(-0.7)	-0.225	5240	0.967	0.955	0.966	0.957
BD + 73 <sup>o</sup> 566	(-1.3)	-0.21	5600		0.904	0.899	0.899
HD 114095	(-1.5)	-0.385	4580	1.113		1.085	1.107
G64 - 12	-3.5	-0.22	6230		0.808	0.806	0.813
BD + 34 <sup>o</sup> 2476	-2.3	-0.22	6210	0.808	0.808	0.816	0.815
HD 123710	(-1.1)	-0.18	5710			0.887	0.879
BD + 26 <sup>o</sup> 2606	(-2.2)	-0.23	5980	0.833	0.838	0.852	0.850
HD 132475	-1.0	-0.22	5550		0.896	0.916	0.912
HD 134169	-1.6	-0.195	5760		0.890	0.862	0.872
BD + 42 <sup>o</sup> 2667	-1.7	-0.21	5960	0.826	0.848	0.862	0.847
HD 144515	(-0.5)	-0.335	4770	1.035		1.075	1.063
HD 158809	(-0.6)	-0.19	5500	0.912		0.911	0.928
BD + 2 <sup>o</sup> 3375	(-2.0)	-0.24	5820	0.854	0.860	0.878	0.872
HD 160693	-0.7	-0.17	5740	0.870		0.882	0.884
HD 161770	(-1.8)	-0.325	4960		1.017	1.023	1.011
BD + 20 <sup>o</sup> 3603	-2.3	-0.16:	6140:		0.829	0.826	0.808
HD 163810	(-1.2)	-0.27:	5270:		0.947	0.940	0.982
HD 175179	(-0.7)	-0.205	5610		0.895	0.887	0.913
HD 181007	(-2.2)	-0.38	4760			1.043	1.076
BD + 26 <sup>o</sup> 3578	-2.3	-0.215	6050		0.825	0.857	0.818
HD 184266	?	-0.235	5340	0.944	0.961	0.961	0.940
HD 188510	-1.8	-0.24	5470	0.931	0.925	0.899	0.928
HD 194598	(-1.4)	-0.19	5850	0.867	0.860	0.868	0.852
HD 210889	(-0.8)	-0.195	5560	0.903		0.906	0.908
BD + 4 <sup>o</sup> 4674	(-0.7)	-0.17	5690	0.895		0.877	0.884
BD + 38 <sup>o</sup> 4955	(-3.0)	-0.30	5080		0.996	0.992	0.987
HD 221950	(-0.6)	-0.14	6170	0.818	0.809	0.837	0.806
HD 222589	(-0.2)	-0.24	5050			1.004	0.994
vB 17	H	-0.14	5450			0.934	0.916
vA 60	H	-0.13	5710			0.884	0.881
vA 79	H	-0.085	6660	0.757	0.759	0.764	0.747
vA 215	H	-0.085	6570		0.767	0.784	0.752
vB 49	H	-0.12	5840			0.864	0.862
vA 315	H	-0.095	6340		0.794	0.814	0.776
vA 548	H	-0.60:	4220:			1.193	1.193
vA 560	H	-0.22	5090			0.994	0.987
vA 625	H	-0.105	6010		0.842	0.844	0.830
vA 692	H	-0.16	5440			0.924	0.930
vA 712	H	-0.24	5030			0.994	1.009
vA 747	H	-0.285	4900			1.024	1.033
vA 748	H	-0.13	5810			0.864	0.872
vA 778	H	-0.23	5080			0.984	0.999

<sup>a</sup>[Fe/H] values in parentheses are estimated from  $\delta(U-B)_{0.6}$  and the calibration of Carney (1979a). "H" stands for Hyades.

We again adopt  $B.C._{\odot} = -0^m12$ . Other choices will simply scale all the results of Table II-1 by the same amount.

In Fig. 10, we display the resultant Hyades and halo dwarf bolometric corrections, confirming the earlier results of CA that the two populations have similar B.C. values for  $T_{\text{eff}} \leq 5000$  K, but that the halo dwarf values

differ from those of Hyades stars by over  $0^m1$  for  $T_{\text{eff}} \geq 6000$  K.

## APPENDIX III: REDDENING

Figures 5(b)-(g) demonstrate the reddening insensitivity of most of the color-color relations used to detect

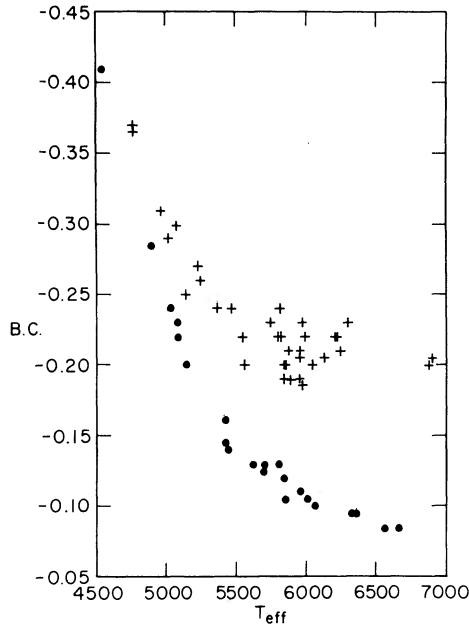


FIG. 10. Empirical bolometric corrections for the single halo dwarfs of Table IV (+) and the single Hyades dwarfs of Table II (•), with data taken from CA and Table VII. A bolometric correction of  $-0^m12$  was adopted for Hyades G2 V stars.

binaries. They may therefore be used to check for unusual flux distributions due to binaries without regard to reddening uncertainties. If the colors are not apparently distorted by a companion, one may then try to compute the reddening using some metallicity-insensitive pair of colors. The best pair for reddening determinations is  $J - K$  vs  $V - K$ , which are shown in Fig. 11 for the single Hyades dwarfs of Paper I and the single halo dwarfs of this paper. The arrow indicates the effects of  $E(B - V) = 0^m1$ . A linear fit for the Hyades stars is

$$(J - K)_0 = 0.270(V - K)_0 - 0^m076, \quad (\text{III-1})$$

while for the halo dwarfs,

$$(J - K)_0 = 0.264(V - K)_0 - 0^m042. \quad (\text{III-2})$$

Given that  $E(J - K) = 0.22 E(B - V)$  and

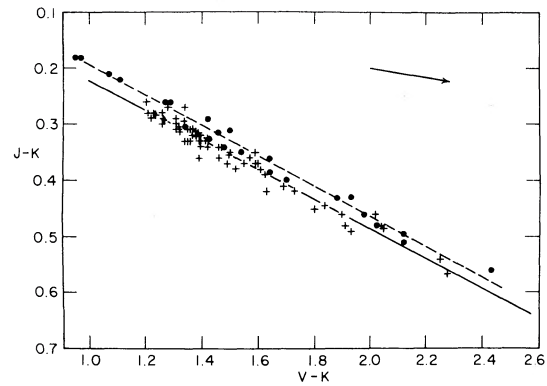


FIG. 11.  $J - K$  vs  $V - K$  for the single halo dwarfs of Table IV (+) and the single Hyades dwarfs of Table II (•). The dashed line is given by Eq. (III-1), and the solid line by Eq. (III-2). The arrow indicates the effects of  $E(B - V) = 0^m1$ .

$E(V - K) = 2.72 E(B - V)$  (Savage and Mathis 1979), we find for Hyades-like stars that

$$E(B - V) = 0.523(V - K) - 1.943(J - K) - 0^m146, \quad (\text{III-3})$$

and that for extremely metal-poor halo dwarfs,

$$E(B - V) = 0.532(V - K) - 2.009(J - K) - 0^m086. \quad (\text{III-4})$$

The method provides a typical accuracy of about  $\pm 0^m03$  in  $E(B - V)$  if the metallicity is approximately known, or about  $\pm 0^m05$  if nothing is known about the metallicity (using a mean of Eqs. III-3 and III-4). In this latter case, however, one may iterate, using the Hyades relation to compute a preliminary reddening, from which obtains  $(U - B)_0$  and  $(B - V)_0$  and hence  $\delta(U - B)_{0.6}$ . If the star is in fact metal-poor relative to the Hyades, a large  $\delta(U - B)_{0.6}$  will result partly because such stars have larger ultraviolet excesses and partly because the Hyades relation will yield an underestimate for  $E(B - V)$ , and reddening acts to increase the observed value of  $\delta(U - B)_{0.6}$ . Iteration should quickly yield proper values.

#### REFERENCES

- Abt, H. A. (1979). *Astron. J.* **84**, 1591.  
 Abt, H. A., and Levy, S. G. (1969). *Astron. J.* **74**, 908.  
 Alden, H. L. (1938). *Astron. J.* **47**, 9.  
 Baade, W. (1944). *Astrophys. J.* **100**, 137.  
 Beardsley, W. R., Gatewood, G., and Kamper, K. W. (1974). *Astrophys. J.* **194**, 637.  
 Bessell, M. S., and Wickramasinghe, D. T. (1979). *Astrophys. J.* **227**, 232.  
 Böhm-Vitense, E., and Johnson, P. (1977). *Astrophys. J. Suppl.* **35**, 461.  
 Bond, H. E. (1980). *Astrophys. J. Suppl.* **44**, 517.  
 Buscombe, W., and Morris, P. M. (1958). *Mem. Mt. Stromlo Obs.*, No. 14.  
 Carney, B. W. (1978a). Ph.D. thesis, Harvard University.  
 Carney, B. W. (1978b). *Astron. J.* **83**, 1087.  
 Carney, B. W. (1979a). *Astrophys. J.* **233**, 211.  
 Carney, B. W. (1979b). *Astrophys. J.* **233**, 877.  
 Carney, B. W. (1980). *Astron. J.* **85**, 38.  
 Carney, B. W. (1982). *Astron. J.* **87**, 1527 (Paper I).  
 Carney, B. W. (1983). *Astron. J.* **88**, 610 (Paper II, preceding paper).  
 Carney, B. W., and Aaronson, M. (1979). *Astron. J.* **84**, 867 (CA).  
 Carney, B. W., and Peterson, R. C. (1981a). *Astrophys. J.* **245**, 238.  
 Carney, B. W., and Peterson, R. C. (1981b). *Astrophys. J.* **251**, 190.  
 Code, A. D., Davis, J., Bless, R. C., and Hanbury Brown, R. (1976). *Astrophys. J.* **203**, 417.  
 Crampton, D., and Hartwick, F. D. A. (1972). *Astron. J.* **77**, 590.  
 Eggen, O. J. (1964). *R. Obs. Bull.*, No. 84.  
 Eggen, O. J. (1969). *Astrophys. J. Suppl.* **19**, 31.

- Eggen, O. J. (1976). *Publ. Astron. Soc. Pac.* **88**, 732.  
Eggen, O. J. (1978). *Astrophys. J. Suppl.* **37**, 251.  
Eggen, O. J. (1979). *Astrophys. J.* **229**, 158.  
Eggen, O. J., Lynden-Bell, D., and Sandage, A. (1962). *Astrophys. J.* **136**, 748.  
Elias, J. H., Frogel, J. A., Matthews, K., and Neugebauer, G. (1982). *Astron. J.* **87**, 1029.  
Frogel, J. A., Persson, S. E., Aaronson, M., and Matthews, K. (1978). *Astrophys. J.* **220**, 75.  
Hanson, R. B. (1979). *Mon. Not. R. Astron. Soc.* **186**, 875.  
Hauck, B., and Mermilliod, M. (1979). *uvby $\beta$  Photoelectric Photometric Catalogue* (Centre de Donnees Stellaires, Strasbourg).  
Johnson, H. L., MacArthur, J. W., and Mitchell, R. I. (1968). *Astrophys. J.* **152**, 465.  
Johnson, H. L., Mitchell, R. I., Iriarte, B., and Wiśniewski, W. Z. (1966). *Comm. Lunar and Planetary Lab.*, **4**, Part 3, 99.  
Kurucz, R. L. (1979). *Astrophys. J. Suppl.* **40**, 1.  
Kurucz, R. L. (1980). Unpublished.  
Lutz, T. E., and Kelker, D. H. (1973). *Publ. Astron. Soc. Pac.* **85**, 573.  
Mayor, J., and Turon, C. (1982). *Astron. Astrophys.* **110**, 241.  
Nicolet, B. (1978). *Homogenized UBV Catalogue* (Centre de Donnees Stellaires, Strasbourg).  
Oort, J. H. (1926). Groningen Publ., No. 40.  
Peterson, R. C., and Carney, B. W. (1979). *Astrophys. J.* **231**, 762.  
Peterson, R. C., Willmarth, D. W., Carney, B. W., and Chaffee, F. H., Jr. (1980). *Astrophys. J.* **239**, 928.  
Popper, D. M. (1942). *Astrophys. J.* **95**, 307.  
Popper, D. M. (1943). *Astrophys. J.* **98**, 209.  
Sandage, A. (1964). *Astrophys. J.* **139**, 442.  
Sandage, A. (1969). *Astrophys. J.* **158**, 1115.  
Savage, B. D., and Mathis, J. S. (1979). *Annu. Rev. Astron. Astrophys.* **17**, 73.  
Schuster, W. J. (1979). *Rev. Mex. Astron. Astrofisica* **4**, 233.  
Trimble, V. L. (1980). I.A.U. Sym. No. 85, *Star Clusters*, edited by J. E. Hesser (Reidel, Boston), p. 259.  
Wallerstein, G. (1976). *Observatory* **96**, 142.  
Worley, C. E. (1969). In *Low-Luminosity Stars*, edited by S. S. Kumar (Gordon and Breach, New York), p. 117.